arXiv:1210.2685v1 [cond-mat.str-el] 9 Oct 2012

XXZ spin-1/2 representation of a finite-U Bose-Hubbard chain at half-integer filling

Domenico Giuliano,[1] Davide Rossini,[2] Pasquale Sodano,[3] and Andrea Trombettoni[4]
[1] *Dipartimento di Fisica, Università della Calabria, Arcavacata di Rende I-87036, Cosenza, Italy & INFN, Gruppo collegato di Cosenza, Arcavacata di Rende I-87036, Cosenza, Italy*
[2] *NEST, Scuola Normale Superiore & Istituto Nanoscienze-CNR, I-56126 Pisa, Italy*
[3] *International Institute of Physics, Universidade Federal do Rio Grande do Norte, 59012-970, Natal, Brazil & INFN, Sezione di Perugia, Via A. Pascoli, I-06123, Perugia, Italy*
[4] *CNR-IOM DEMOCRITOS Simulation Center and SISSA, Via Bonomea 265 I-34136 Trieste, Italy & INFN, Sezione di Trieste, I-34127 Trieste, Italy*

Using a similarity Hamiltonian renormalization procedure, we determine an effective spin-1/2 representation of the Bose-Hubbard model at half-integer filling and at a finite on-site interaction energy U. By means of bosonization, we are able to recast the effective Hamiltonian as that of a spin-1/2 XXZ magnetic chain with pertinently renormalized coupling and anisotropy parameters. We use this mapping to provide analytical estimates of the correlation functions of the Bose-Hubbard model. We then compare such results with those based on DMRG numerical simulations of the Bose-Hubbard model for various values of U and for a number L of lattice sites as low as $L \sim 30$. We find an excellent agreement up to 10% between the output of analytical and numerical computations, even for relatively small values of U. Our analysis implies that, also at finite U, the 1D Bose-Hubbard model with suitably chosen parameters may be seen as a quantum simulator of the XXZ chain.

PACS numbers: 75.10.Pq, 75.10.Jm, 67.85.-d

I. INTRODUCTION

The study of magnetic systems is one of the more active fields of research in condensed matter physics[1]: the variety of emerging ground-states, as well as the rich phase diagram of magnetic lattices, makes these systems an optimal testbed where it is possible to study the competition between various orders and frustration effects[2]. From this perspective, it would be very useful to be able to engineer synthetic physical systems effectively describing magnetic model Hamiltonians, with tunable geometry and parameters.

A promising route is provided by cold atoms setups: for instance, itinerant magnetism in bulk ultracold Fermi systems with repulsive interactions has been experimentally studied[3], while small spin networks have been simulated with ion chains[4]. Effective nearest-neighbour spin-spin interactions for atoms in neighbour wells of an optical lattice may result from super-exchange couplings: the corresponding second-order tunneling has been observed in array of double wells[5]. Furthermore, using fast oscillations of the optical lattice, one can control the sign of the nearest-neighbour tunneling[6], which has been recently used to simulate classical frustrated magnetism in triangular lattices[7]. Finally, in ultracold atomic systems one may use two-component gases: here, the two internal degrees of freedom correspond to the simulated (pseudo)spins. In optical lattices, in the regime of strong interactions, by adjusting the external potential one can control spin interactions between spin states of neighbouring atoms[8]. The recent experimental realization of controllable Bose-Bose mixtures[9] then paves the way towards the experimental simulation of spin Hamiltonians, in which the atomic counterpart of magnetic phases, like the antiferromagnetic Néel and the XY ferromagnetic phases (corresponding respectively to the checkerboard and the supercounterfluid phases[10]) may be detected and studied.

A key tool in the manipulation of ultracold atomic systems is the possibility to superimpose and control optical lattices[11]. The low-energy properties of ultracold bosons in deep optical lattices are well captured by the Bose-Hubbard (BH) Hamiltonian[12]

$$H_{\rm BH} = \sum_{\langle i,j \rangle} \left[-t(b_i^\dagger b_j + b_j^\dagger b_i) + V n_i n_j \right] + \frac{U}{2} \sum_i n_i (n_i - 1) \, . \tag{1}$$

In Eq. (1), i, j denote the lattice sites, while $\langle i,j \rangle$ stands for any pair of nearest neighbouring sites. The operators $b_i^\dagger$ (b_i), with $[b_i, b_j^\dagger] = \delta_{i,j}$ and $n_i = b_i^\dagger b_i$, create (annihilate) a boson in the site i. The parameter t denotes the hopping strength, and U (V) is the interaction energy of two particles at the same site (at two nearest neighbouring sites).

The use of optical lattices in ultracold atomic systems is also central in other proposals to simulate spin Hamiltonians: in Ref. 13 it was suggested to use spinor Bose gases in optical lattices to implement the quadratic-biquadratic spin Hamiltonian. The mapping of a Mott insulator of one-component ultracold bosonic gases in a tilted 1D optical lattice onto a spin Hamiltonian was discussed in Ref. 14. Based on this proposal, the quantum simulation of an antiferromagnetic spin chain (more precisely, an Ising model in a transverse field[15]) has been experimentally demonstrated[16]: varying the effective magnetic field, a quantum phase transition occurs between a paramagnetic phase and an antiferromagnetic one. These phases (and the corresponding phase transition) were detected by measuring the probability to have an odd occupation of sites, while the formation of magnetic domains was observed using in-situ site-resolved imaging and noise correlation measurements[16].

Apart from the simulation of quantum magnetism, more generally the possibility of realizing BH models[17] through the use of ultracold atoms in optical lattices[12] attracted a huge interest in the last decade for a number of other reasons: the experimental detection of the Mott-superfluid transition[18] motivated a thorough study of the quantum phases of the BH model. From this point of view, arrays of ultracold atoms are versatile synthetic systems for the study of strongly interacting lattice systems[19,20] in which it is possible to investigate a huge variety of phenomena, ranging from quantum phase transitions[11] to superfluid dynamics in lattices[21] and non-equilibrium dynamics of quantum systems[22].

For very large values of U, i.e. for $t/U \ll 1$, the BH model may be mapped into the Heisenberg XXZ spin-1/2 Hamiltonian

$$H_{\rm XXZ} = -J \sum_{\langle i,j \rangle} \left(s_i^x s_j^x + s_i^y s_j^y - \Delta s_i^z s_j^z \right), \qquad (2)$$

where $\vec{s}_i = \vec{\sigma}_i/2 = (s_i^x, s_i^y, s_i^z)$ are the $S = 1/2$ spin operators, $\vec{\sigma}_i$ being the Pauli matrices, J is the nearest-neighbour coupling, and Δ is the anisotropy parameter ($\Delta = \pm 1$ respectively correspond to the antiferromagnetic and the ferromagnetic isotropic Heisenberg model).

The use of lattice spin systems for interacting bosons traces back to the classical papers by Matsubara and Matsuda in the 50's[23]. In those papers the properties of helium II are studied assuming that each atom in liquid helium can occupy one of the lattice points: this assumption naturally leads to a (BH-like) lattice Hamiltonian. The further assumption that two atoms cannot simultaneously occupy the same lattice site (due to the hard-core part of the interparticle interaction between Helium atoms[24] or, in BH language, by a an infinite U) leads to a XXZ spin-1/2 model in a magnetic field[23]. To qualitatively understand the emergence of a spin representation of the one-component BH model one may say that, when $U \to \infty$ and *if* two states per site give a dominant contribution to the energy, an XXZ Hamiltonian is retrieved: this is exactly what happens when the filling f, defined as the average number of bosons per lattice site, is half-integer. Indeed, when $f = \bar{n} + 1/2$, with $\bar{n}$ integer, the relevant states in the Fock space are given by $|\bar{n}\rangle$ and $|\bar{n}+1\rangle$ (deviations from half-integer fillings would result in a magnetic term in the XXZ Hamiltonian). For half-integer f, at the leading order in $t/U \to 0$ one has $J = 2t(f + 1/2)$ and $\Delta = V/J$ (see the discussion in Section III).

The XXZ model is a paradigmatic spin Hamiltonian which has been the object of many investigations (see e.g. Ref. 25) and that in 1D is exactly solvable by Bethe ansatz[26–28]; this provides an ideal arena to test different analytical and numerical techniques, from bosonization[29,30] to density matrix renormalization group (DMRG)[31]. The study of (static and dynamical) correlation functions in this model is currently an active area of research[32–41] and exact analytical results for the correlation functions at small distance (both at zero and finite temperature) are by now available[34]. The asymptotic form of the ground-state correlation functions in the thermodynamic limit is power-law with an exponent that has been obtained by comparing the result of abelian bosonization with the Bethe ansatz solution[42]: for an open chain in the region $-1 \leq \Delta \leq 1$, the numerical findings for correlation functions obtained with DMRG were compared with the results of a low-energy field theory, showing a very good agreement and allowing for precise estimates of the amplitudes of the correlation functions[43]. In turn, the obtained amplitudes were found in agreement with the analytical expressions given by Lukyanov and Zamolodchikov[44,45]. Finally, exact results obtained for the XXZ chain in a special scaling limit were used to compute the local correlations of a continuous Lieb-Liniger 1D Bose-gas[46].

In this paper we determine a correspondence between the BH chain at half-integer filling for *finite* U and a 1D XXZ spin-1/2 model. This enables us to provide analytical expressions for the BH correlation functions, which we compare with numerical results obtained with DMRG, showing that there is a very good agreement both at large and small distances and also for U/J as low as ~ 2 and for a number of sites $L \geq 30$. As a consequence, the numerical determination of the phase transitions superfluid-charge density wave and superfluid-Mott insulator (respectively corresponding, in the effective XXZ chain, to $\Delta_{\rm eff} = 1$ and $\Delta_{\rm eff} = -1$) well agrees with the analytical results for the XXZ chain. Besides providing a way to an analytical study of the quantum phase transitions of the BH model, our analysis may reveal very useful in determining the structure factor as well as the response of the BH chain to external perturbations. As a result, we are able not only to provide analytical expressions for 1D BH correlation functions, but also to show that by realizing the 1D BH chain at half-integer filling one can provide a quantum simulation of the XXZ chain.

In the following we shall derive an effective spin-1/2 Hamiltonian for the BH chain at half-integer filling as a power series of t/U. Following Refs. 47,48, we perform a continuous unitary transformation $\mathbf{S}$ which block-diagonalizes the BH Hamiltonian in the basis of the eigenvectors of $H_{\rm BH}$ with $t = 0$. The latter requirements yields an equation for $\mathbf{S}$ which we solve perturbatively to the order $(t/U)^2$. We finally show that, using bosonization, this Hamiltonian can be recasted in the XXZ form with pertinent coupling and anisotropy parameters. We observe that, while to the first order in t/U one finds a XXZ model with $J = 2t(f + 1/2)$ and $\Delta = V/J$, to the next order in t/U one gets an effective spin Hamiltonian which is not of the XXZ form, since it contains also next-nearest neighbours and 3-spin terms (this is the bosonic counterpart of a similar computation done for the 2D Fermi-Hubbard model[49,50], where 4-spin terms appear). However, in 1D it is possible to further proceed using bosonization: we do this for the BH chain, where one can obtain analytical results introducing a Luttinger liquid description of the effective Hamiltonian enabling to incorporate the long-wavelength behaviour of non-XXZ terms in the effective coupling and anisotropy parameters, $J_{\rm eff}$ and $\Delta_{\rm eff}$, which are now function of t, V, f *and* U.

The plan of the paper is the following: in Section II we introduce the BH and the XXZ models, recalling some useful properties and results. In Section III we employ the continuous unitary transformation introduced by Glazek and Wilson[47] to approximate the BH chain at half-integer filling with an effective spin-1/2 effective Hamiltonian. In Section IV we use bosonization to recast this effective Hamiltonian as an XXZ Hamiltonian, with effective coupling $J_{\rm eff}$ and anisotropy $\Delta_{\rm eff}$. In Section V we establish the correspondence between the correlation functions of the BH model and the ones of the XXZ chain. The results of Section III-V are then used to compare the analytical results obtained for the BH chain correlation functions with the numerical findings obtained by DMRG numerical simulations: the results of this comparison are detailed in Section VI, both for the correlation functions and the phase transition points. Section VII is devoted to our conclusions, while more technical details are contained in the Appendices.

II. MODEL HAMILTONIANS

In this Section we review the basic properties of the BH and of the spin-1/2 XXZ Hamiltonians, in particular focusing on known analytical results about the real space spin correlations in the XXZ chain.

A. Bose-Hubbard model

The low-energy properties of interacting bosons in a one-dimensional deep optical lattice are in general well described by the Bose-Hubbard Hamiltonian (1), which, in 1D and with open boundaries, reads:

$$\begin{aligned} H_{\rm BH} &= -t\sum_{i=1}^{L-1}\left(b_i^\dagger b_{i+1}+b_{i+1}^\dagger b_i\right)+\frac{U}{2}\sum_{i=1}^{L} n_i\left(n_i-1\right) \\ &+ V\sum_{i=1}^{L-1} n_i n_{i+1}. \end{aligned} \tag{3}$$

We denote with N the total number of particles in the L-site chain, so that the filling f, that is, the average number of particles per site, is given by $f=\frac{N}{L}$. For alkali atoms usually $V \ll U$, but with dipolar gases (or polar molecules) V could be comparable with U: experiments with dipolar gases[51] and long-lived ground-state polar molecules[52] in optical lattices have been already performed (see also the review 53).

A large amount of experiments investigated the properties of the BH model: the main reason for this interest lies on the fact that this model exhibits a quantum phase transition between a superfluid phase (for $t/U \gg 1$) and a Mott insulator (for $t/U \ll 1$)[17]. A finite V generally favours charge density wave phases: e.g., for half-integer filling $f=1/2$, a large $V \gg t, U$ will result in a ground-state of the type $|1,0,1,0,\cdots\rangle$ (where in general $|n_1,n_2,n_3,\cdots\rangle$ is an eigenfunction of $H_{\rm BH}$ with $t=0$). The ground-state of the BH model has been studied in the seminal paper in Ref. 17 using the grand-canonical ensemble, where the chemical potential μ is introduced to enforce the constraint on the number of particles. The phase diagram in the $U-\mu$ plane shows the characteristic lobes[17]: for a pertinently fixed value of μ the half-integer fillings may be made correspond to the "basis" of the lobes (i.e. where the lobes touch) and, for $V=0$, one has a superfluid for each finite value of t, while a finite and positive value of V gives rise to a charge density wave region among the Mott lobes.

The Mott-insulator/superfluid transition was first observed in 3D[18] and subsequently in 1D[54] and 2D[55]. The effect of a superimposed external potential (typically a parabolic one) has been also considered: the so-called wedding-cake-like density has been studied both theoretically[56,57] and experimentally[58,59]. The phase coherence properties of ultracold bosons in optical lattices have been studied, as well, showing that phase coherence on short length scales still persists deep in the insulating phase[60]. The BH model in a 1D geometry can be obtained either by tightly confining the bosonic cloud in two radial directions in presence of a periodic potential in the transverse direction, or by creating many (eventually uncoupled) tubes with a 2D optical lattice. The Bragg spectroscopy of interacting one-dimensional Bose gases loaded in an optical lattice across the superfluid to Mott-insulator phase transition has been performed and the properties of the strongly correlated phases investigated looking at the Bragg spectra[61]. The excitation spectrum in the strongly interacting regime has been studied also in presence of a tunable disorder, created by a bichromatic optical lattice, showing a broadening of the Mott-insulator resonances[62].

The finite-V 1D BH model has been studied with a number of analytical and numerical techniques: in particular in Ref. 63 the phase boundaries of the Mott insulators and charge density wave phases were determined by DMRG. The zero-temperature phase diagram both of the BH model and of a spin-S Heisenberg model was constructed and their relation investigated[64]. The role of V in inducing supersolid phases in the 1D BH model was also studied[65–68]. Bosonization techniques quite generally provide in 1D a very effective way to compute the correlation functions and their decay at large distance: thus, they have been applied as well to 1D BH chains (see the review 69).

Finally, we mention that the effect of intersite interactions was considered since the 90's in a related model, the quantum phase model, describing Josephson junction arrays[70]: the quantum phase model can be obtained from the BH model for large filling per site when the number fluctuations are negligible in the kinetic term. In the correspondence between the two models the chemical potential μ term in the BH model corresponds to the so-called "offset charge" q, which are external charges present in the superconducting network[70]: the lobes in the quantum phase model are equal, since there is an invariance for $q \to q + 2e$ ($2e$ being the charge of the Cooper pairs), and an half-integer value of the filling f corresponds to half-integer values of the offset charges $q/2e$. The study of intersite interactions is relevant in Josephson junction arrays since the interaction term depends on the capacitance matrix C_{ij}, which is in general not diagonal, resulting in terms of the form $V_{ij} n_i n_j$, where $V_{ij} \propto (C_{ij})^{-1}$: as a mean-field analysis shows[71], for a diagonal capacitance matrix one has that at $T = 0$ the superconducting phase is obtained for each value of the Josephson energy E_J ($\propto t$ in the mapping) and that at $q = e$ one has a finite critical temperature for the Mott-insulator/superfluid transition for each finite value of E_J (unlike $q = 0$, where a critical value of E_J is required). Non-diagonal terms of the capacitance matrix favour charge density waves[70]: the role of the intersite terms was considered for superconducting chains and the corresponding phase diagram investigated[72,73], revealing that in 1D a (superconducting) repulsive Luttinger liquid phase exists.

To conclude this Section let us mention that, in the rest of the paper, we will mostly deal with half-integer fillings, $f \equiv \bar{n} + \frac{1}{2}$, with $\bar{n} = 0, 1, 2, \cdots$. The reason for such a choice is that in this case the relevant states for the description of system for $U \to \infty$ are just $|\bar{n}\rangle$ and $|\bar{n}+1\rangle$. Simple arguments - reviewed in Section II B - then show that, to first order in t/U, the BH Hamiltonian is mapped into an XXZ spin-1/2 Hamiltonian which is integrable in 1D. Within the XXZ-model framework, it is also possible to consider small deviations from the half-filled regime, which mainly give rise to a uniform magnetic field in the z-direction. Even though we will not consider large fluctuations in f (of order 1), it is possible to take them into account, by keeping, as relevant states for $U \to \infty$, $|\bar{n}\rangle$, $|\bar{n}-1\rangle$, $|\bar{n}+1\rangle$. In this case, an effective spin-1 XXZ effective model (in general not integrable) is expected[74]. Spin-1 models exhibit a gapped (Haldane) insulator phase[75,76], which has been investigated in the context of the 1D BH model[77–81].

B. XXZ chain

For a chain with L sites and open boundaries, the Hamiltonian of a spin-1/2 XXZ model given in Eq. (2) particularizes to:

$$H_{\mathrm{XXZ}} = -J \sum_{i=1}^{L-1} \left(s_i^x s_{i+1}^x + s_i^y s_{i+1}^y - \Delta s_i^z s_{i+1}^z \right). \qquad (4)$$

The global minus sign in the couplings has been introduced in order to more easily perform the comparison with the BH model, and it can be readily gauged away by implementing the canonical mapping to the spin-1/2 operators τ_j^a defined as $\tau_j^{x,y} = (-1)^j s_j^{x,y}$, $\tau_j^z = s_j^z$. Therefore the chain is antiferromagnetic (ferromagnetic) for Δ positive (negative).

Following Ref. 23, one can derive the Hamiltonian in Eq. (4) from the BH Hamiltonian (3) at half-integer filling f and for $U \to \infty$. To do so, let us define $s_j^z \equiv n_j - f$ (so that the eigenvalues of s_j^z are $\pm\frac{1}{2}$). Since for $t = 0$ the energy per particle is (for $L \to \infty$) $\varepsilon = Uf(f-1)/2 + Vf^2$, it follows that $H_{\mathrm{BH}} \xrightarrow{t\to 0} V s_j^z s_{j+1}^z$, i.e.

$$J\Delta \equiv V. \qquad (5)$$

Similarly, for $f \gg 1$, one gets $J \approx 2tf$ as one can see by putting $b_i \sim \sqrt{f} e^{i\phi_i}$ and mapping the obtained result in the XXZ spin-1/2 language[72]: for finite values of f one gets (see Section III)

$$J \equiv 2t\left(f + \frac{1}{2}\right). \qquad (6)$$

Eqs. (5) and (6) provide the desired mapping between the BH model and the XXZ Hamiltonian to lowest order in t/U. However, as we are going to see in Section V, to get a quantitative agreement between the BH and the XXZ correlation functions even for t/U relatively small (as low as 0.1 for $f = 1/2$) one has to go to the next order in t/U: the corresponding Hamiltonian is determined in Section III and recasted in XXZ form via a Luttinger representation in Section IV. We remark that, since our result are obtained at half-integer filling, we may omit the addition of a magnetic field term of the form $\propto \sum_{i=1}^{L} s_i^z$ to Eq. (4). Indeed such a term is proportional to the total spin $S_T^z = \sum_{i=1}^{L} s_i^z$ in the z direction and, since the system is half-filled, only eigenstates of H_{XXZ} with $S_T^z = 0$ are physically meaningful - notice that in the following analytical results based on the XXZ Hamiltonian (4) are compared with numerical DMRG simulations of the BH chain in the canonical ensemble, where $\sum_i n_i$ is conserved and equal to N.

The Hamiltonian H_{XXZ} is exactly solvable by means of standard Bethe ansatz techniques[26–28]: however, explicitly computing the real space spin-spin correlation functions is quite a difficult task. Exact analytical results for short-range correlators in a range of up to seven lattice sites were reported for the isotropic Heisenberg model in Ref. 40, in the thermodynamic limit ($L \to \infty$) and at arbitrary finite temperature, and for finite chains of arbitrary length L in the ground-state. Results for short-range correlation functions are also available for the XXZ chain[34]. For large distances, using the standard bosonization approach[29,30] to spin-1/2 XXZ model[82], one may find out all the spin-spin correlation functions in terms of two-point correlators of pertinent conformal operators[43]: in the thermodynamic limit one finds the asymptotic forms

$$\begin{aligned}\langle\psi_0|s_i^z s_j^z|\psi_0\rangle &= (-1)^{i-j}\frac{A_z}{|i-j|^{1/\eta}} - \frac{1}{4\pi^2\eta\,(i-j)^2},\\ \langle\psi_0|s_i^x s_j^x|\psi_0\rangle &= (-1)^{i-j}\frac{A_x}{|i-j|^{\eta}} - \frac{\tilde{A}_x}{|i-j|^{\eta+1/\eta}}, \qquad (7)\end{aligned}$$

where $|\psi_0\rangle$ is the ground-state of $H_{\rm XXZ}$ and we set[42]

$$\eta = 1 - \frac{1}{\pi}\arccos\Delta. \qquad (8)$$

Analytical expressions for the correlation amplitudes A_x, $\tilde{A}_x$ and A_z entering Eqs. (7)-(7) were presented in Refs. 44,45 and further discussed in Ref. 83 (see also the discussion in Section V of Ref. 41):

$$\begin{aligned}A_x &= \frac{\mathcal{A}^{\eta}}{8(1-\eta)^2}\,e^{-\mathcal{I}_x}; \qquad (9)\\ \tilde{A}_x &= \frac{\mathcal{A}^{\eta+1/\eta}}{2\eta(1-\eta)}\,e^{-\tilde{\mathcal{I}}_x}; \qquad (10)\\ A_z &= \frac{2\mathcal{A}^{1/\eta}}{\pi^2}\,e^{\mathcal{I}_z} \qquad (11)\end{aligned}$$

with

$$\mathcal{I}_x = \int_0^\infty \frac{dt}{t}\left(\frac{\sinh(\eta t)}{\sinh(t)\cosh[(1-\eta)t]} - \eta e^{-2t}\right)$$

$$\tilde{\mathcal{I}}_x = \int_0^\infty \frac{dt}{t}\left(\frac{\cosh(2\eta t)e^{-2t}-1}{2\sinh(\eta t)\sinh(t)\cosh[(1-\eta)t]} + \frac{1}{\sinh(\eta t)} - \frac{\eta^2+1}{\eta}e^{-2t}\right),$$

$$\mathcal{I}_z = \int_0^\infty \frac{dt}{t}\left(\frac{\sinh[(2\eta-1)t]}{\sinh(\eta t)\cosh[(1-\eta)t]} - \frac{2\eta-1}{\eta}e^{-2t}\right)$$

and

$$\mathcal{A} = \frac{\Gamma\left(\frac{\eta}{2(1-\eta)}\right)}{2\sqrt{\pi}\,\Gamma\left(\frac{1}{2(1-\eta)}\right)}, \qquad (12)$$

and $\Gamma(x)$ being the Euler's Gamma function.

Analytical expressions (in the large-L limit) for the subsequent prefactors of the correlation functions are reported in Refs. 36,41.

For chains of finite size L with open boundary conditions, one obtains[43]:

$$\begin{aligned}\langle\psi_0|s_i^z s_j^z|\psi_0\rangle &= \frac{(-1)^{i-j}a^2}{2f_{\frac{1}{2\eta}}(2i)f_{\frac{1}{2\eta}}(2j)}\left(\frac{f_{\frac{1}{\eta}}(i+j)}{f_{\frac{1}{\eta}}(i-j)} - \frac{f_{\frac{1}{\eta}}(i-j)}{f_{\frac{1}{\eta}}(i+j)}\right) - \frac{1}{4\pi^2\eta}\left(\frac{1}{f_2(i-j)} + \frac{1}{f_2(i+j)}\right)\\ &\quad - \frac{a}{2\pi\eta}\left\{\frac{(-1)^i}{f_{\frac{1}{2\eta}}(2i)}[g(i-j)+g(i+j)] - \frac{(-1)^j}{f_{\frac{1}{2\eta}}(2j)}[g(i-j)-g(i+j)]\right\} \qquad (13)\end{aligned}$$

and

$$\begin{aligned}\langle\psi_0|s_i^x s_j^x|\psi_0\rangle &= \frac{f_{\frac{\eta}{2}}(2i)f_{\frac{\eta}{2}}(2j)}{f_\eta(i-j)f_\eta(i+j)}\left\{(-1)^{i-j}\frac{c^2}{2} - \frac{b^2}{4f_{\frac{1}{2\eta}}(2i)f_{\frac{1}{2\eta}}(2j)}\left[\frac{f_{\frac{1}{\eta}}(i+j)}{f_{\frac{1}{\eta}}(i-j)} + \frac{f_{\frac{1}{\eta}}(i-j)}{f_{\frac{1}{\eta}}(i+j)}\right]\right.\\ &\quad \left. - \frac{bc}{2}\,\mathrm{sgn}(i-j)\left[\frac{(-1)^i}{f_{\frac{1}{2\eta}}(2j)} - \frac{(-1)^j}{f_{\frac{1}{2\eta}}(2i)}\right]\right\}, \qquad (14)\end{aligned}$$

where $\mathrm{sgn}(x)$ is the sign function and

$$\begin{aligned}f_\alpha(x) &= \left[\frac{2(L+1)}{\pi}\sin\left(\frac{\pi|x|}{2(L+1)}\right)\right]^\alpha, \qquad (15)\\ g(x) &= \frac{\pi}{2(L+1)}\cot\left(\frac{\pi x}{2(L+1)}\right) \qquad (16)\end{aligned}$$

with

$$\frac{c^2}{2} \equiv A_x, \quad \frac{b^2}{4} \equiv \tilde{A}_x, \quad \frac{a^2}{2} \equiv A_z \qquad (17)$$

(here and in the following all the distances are in units of the lattice constant).

The agreement between exact numerical calculations of the XXZ correlation functions and analytical expressions in (13)-(14) is very good, and it becomes excellent with $L \sim 100$ for $-0.8 \lesssim \Delta \lesssim 0.8$[43]. Thus one may readily assume that Eqs. (13)-(14) provide quite an accurate analytical expression for the spin-spin correlation functions in the XXZ model[84]. As a consequence, constructing a rigorous mapping between the BH and the XXZ spin-1/2

Hamiltonian and expressing correlation functions in one model in terms of the ones of the other gives an efficient and straightforward way to provide accurate analytic expressions for real space correlation functions in the BH model at half-integer filling.

We finally observe that the only system-dependent parameter determining the spin-spin correlation functions is the coefficient η: thus, in tracing out the mapping between the two models, this is the key quantity to be calculated as a function of the BH parameters. In particular, one may distinguish between the regions in parameter space with $\eta > 1/2$ and $\eta < 1/2$: while the former one corresponds to an antiferromagnetic spin chain, the latter one (which may be realized for pertinently chosen values of the parameters of $H_{\rm BH}$, as we shall show below) corresponds to a ferromagnetic chain.

III. EFFECTIVE SPIN-1/2 HAMILTONIAN FOR THE BOSE-HUBBARD MODEL AT HALF-INTEGER FILLING

As reviewed in the previous Section, for $U \to \infty$, the BH Hamiltonian maps onto the XXZ model in Eq. (4), with the parameters J, Δ given in Eqs. (5, 6). This may be seen as a first-order term in an expansion (in powers of t/U) aimed at computing the effective Hamiltonian: in this Section we compute this effective Hamiltonian to the next order. As we shall show in the following, this is enough to fit quite well the numerical data for the correlation functions of the BH model using the analytical results obtained for the correlators of the XXZ chain.

To approach the large-U limit one may either proceed by performing a strong coupling expansion to the second-, or higher-order of perturbation theory, or by deriving effective Hamiltonians using alternative techniques, based on canonical transformations or continuous unitary transformations[85]. Strong coupling techniques were extensively applied to the BH model at integer filling: as a result, one may, for instance, evaluate the energy of the Mott insulator and of the superfluid state in higher-order perturbation theory and determine the phase transition point and the phase diagram in the $U - \mu$ plane[86]. Since we are rather interested to the BH at half-integer filling, i.e., in the region of the phase diagram where the lobes touch and the superfluid phase persists also at very small U (with $V = 0$), we found it convenient to use an approach based on continuous unitary transformations[47,48]. We follow the notation and the method presented in the paper by Glazek and Wilson (GW)[47]: systematically using the GW renormalization procedure, we work out an effective description of the dynamics of the BH model, restricted to the low-energy subspace determined by the constraint on the total number of particles and by the large-U assumption. As a result, the low-energy subspace is spanned by states with either $\bar{n}$ or $\bar{n}+1$ particles per site, with the total number of particles being fixed to N. Thus, the space of physically relevant states at each site is in one-to-one correspondence with the Hilbert space of states of a quantum spin-1/2 degree of freedom; we shall see that, at half-integer filling, even for finite U the BH model may be replaced by an effective spin-1/2 Hamiltonian, with pertinently determined parameters. The method amounts to an iterative block-diagonalization of the BH Hamiltonian on the space of eigenfunctions of $H_{\rm BH}$ with $t = 0$.

To illustrate the procedure, we start from the explicit construction of the “low-energy” Hilbert space of physically relevant states, in the large-U limit. Neglecting excitations with energy $\sim U$ amounts to truncating the Hilbert space to a subspace $\mathcal{F}$, defined as

$$\mathcal{F} = {\rm Span}\{|\bar{n} + \mu_1, \dots, \bar{n} + \mu_L\rangle\}, \tag{18}$$

with μ_i taking the values $\mu_i = 0, 1$ and $\sum_{i=1}^{L} \mu_i = \frac{L}{2}$. In Eq. (18) $|n_1, \cdots, n_L\rangle$ labels the state in the Hilbert space with n_i particles on site i. To implement the GW approach, one splits the Hamiltonian (3) as $H_{\rm BH} = H_0 + H_I$, with

$$\begin{aligned} H_0 &= \frac{U}{2} \sum_i n_i(n_i - 1) + V \sum_i n_i n_{i+1} & (19) \\ H_I &= -t \sum_i \left(b_i^\dagger b_{i+1} + b_{i+1}^\dagger b_i \right). & (20) \end{aligned}$$

From Eqs. (19)-(20) one sees that H_0 is diagonal with respect to the partition of the Hilbert space into $\mathcal{F}$ plus its orthogonal complement, since

$$H_0|n_1, \dots, n_L\rangle = E_0[n_1, \dots, n_L]|n_1, \dots, n_L\rangle \tag{21}$$

with $E_0[n_1, \dots, n_L] = (U/2) \sum_i n_i(n_i - 1) + V \sum_i n_i n_{i+1}$, while H_I exhibits off-diagonal (with respect to the partition of the Hilbert space) matrix elements which are $\mathcal{O}(t\bar{n})$. In order to block-diagonalize $H_{\rm BH}$, one needs to perform a *similarity* transformation[47]

$$H_{\rm BH} \to \tilde{\mathcal{H}}_{\rm BH} = \mathbf{S}^\dagger H_{\rm BH} \mathbf{S}, \tag{22}$$

with $\mathbf{S}$ unitary. Upon setting $\mathbf{S} = \mathbf{I} + \mathbf{T}$, the unitarity of $\mathbf{S}$ implies the optical theorem

$$\mathbf{T} + \mathbf{T}^\dagger + \mathbf{T}^\dagger \mathbf{T} = 0. \tag{23}$$

Setting $\mathbf{T} \equiv \mathbf{h} + \mathbf{a}$, with

$$\mathbf{h} = \frac{1}{2}\left(\mathbf{T} + \mathbf{T}^\dagger\right), \;\; \mathbf{a} = \frac{1}{2}\left(\mathbf{T} - \mathbf{T}^\dagger\right) \tag{24}$$

one finds that Eq. (23) yields

$$\mathbf{h} = \frac{1}{2}(\mathbf{a}^2 - \mathbf{h}^2). \tag{25}$$

Eq. (25) shows that $\mathbf{h}$ is always “higher order” than $\mathbf{a}$. Following Ref. 47, it is most convenient to define the new interaction Hamiltonian $\tilde{\mathcal{H}}_I$ as

$$\tilde{\mathcal{H}}_I = \tilde{\mathcal{H}}_{\rm BH} - H_0 \tag{26}$$

so that the new "free" Hamiltonian is the same as the old one (H_0).

To further proceed and determine $\mathbf{S}$, one has to require that the matrix elements of $\tilde{\mathcal{H}}_I$ between states with energy difference $\gtrsim U$ are equal to zero, amounting to state that $\tilde{\mathcal{H}}_I$ is block-diagonal with respect to the partition of the Hilbert space into $\mathcal{F}$ plus its orthogonal complement, i.e.

$$\mathcal{P}\tilde{\mathcal{H}}_I\mathcal{P} + (\mathbf{I}-\mathcal{P})\,\tilde{\mathcal{H}}_I\,(\mathbf{I}-\mathcal{P}) = \tilde{\mathcal{H}}_I, \tag{27}$$

where $\mathcal{P}$ is the projector onto $\mathcal{F}$ and $\mathbf{I}-\mathcal{P}$ the projector onto its complementary subspace[87]. One sees that Eq. (27) implies that

$$\mathcal{P}\tilde{\mathcal{H}}_I\,(\mathbf{I}-\mathcal{P}) = (\mathbf{I}-\mathcal{P})\,\tilde{\mathcal{H}}_I\mathcal{P} = 0. \tag{28}$$

Using Eqs. (22)-(24)-(26), one may write $\tilde{\mathcal{H}}_I$ as

$$\tilde{\mathcal{H}}_I = (\mathbf{I}+\mathbf{h}-\mathbf{a})\,(H_0+H_I)\,(\mathbf{I}+\mathbf{h}+\mathbf{a}) - H_0 \tag{29}$$

and Eq. (28) then becomes

$$\begin{aligned}\mathcal{P}\{H_I + \{H_0,\mathbf{h}\} + [H_0,\mathbf{a}] + \mathbf{T}^\dagger H_I + H_I\mathbf{T}\\ + \mathbf{T}^\dagger H_I\mathbf{T}\}\,(\mathbf{I}-\mathcal{P}) = 0.\end{aligned} \tag{30}$$

Eq. (30), together with the identity

$$\mathbf{a} = \mathcal{P}\mathbf{a}\,(\mathbf{I}-\mathcal{P}) + (\mathbf{I}-\mathcal{P})\,\mathbf{a}\mathcal{P} \tag{31}$$

and with Eq. (25), is all what one needs in principle to fully determine $\mathbf{a}$ and $\mathbf{h}$ (and, therefore, the operator $\mathbf{T}$).

However, except for some simple cases[48], an explicit solution for $\mathbf{T}$ cannot be exhibited. For this reason we proceed by writing the solution for $\mathbf{T}$ iteratively, in a series in H_I: in particular, we use Eq. (30) to determine $\mathbf{a}$ to first order ($\mathbf{a_1}$) in H_I. We provide the details in Appendix A and the result for $\mathbf{a_1}$ in Eq. (A4). Using Eq. (A4) and setting $\mathbf{T} \approx \mathbf{a_1}$, we find that Eq. (22) reads as

$$\mathbf{S}^\dagger H_{\rm BH}\mathbf{S} = H_{\rm BH} + [H_0,\mathbf{a_1}] + [H_I,\mathbf{a_1}]. \tag{32}$$

The GW procedure may be readily iterated to determine, in principle, $\mathbf{T}$ to any desired order in H_I. However, since keeping only second-order contributions in H_I provides already quite an excellent estimate for the real-space correlation functions of operators in the BH model (as explicitly shown by the numerical calculations we report in Section VI), setting $\mathbf{T} \approx \mathbf{a_1}$ already provides quite a good approximation to the exact $\mathbf{T}$.

Since the approach we are implementing is perturbative in H_I, one should enforce Eq. (30), as well as Eq. (31), to each order in H_I; moreover, since $\mathcal{P}[H_0,\mathbf{a_1}]\mathcal{P} = 0$, one may neglect the term $[H_0,\mathbf{a_1}]$ in Eq. (32) and approximate the effective Hamiltonian acting within $\mathcal{F}$ as

$$H_{\rm eff} = \mathcal{P}\,\{H_{\rm BH} + [H_I,\mathbf{a_1}]\}\,\mathcal{P} \equiv H^{(0)}_{\rm XXZ} + H^{(1)}. \tag{33}$$

The first term in the right hand side of Eq. (33) yields a spin-1/2 Hamiltonian which is actually the spin-1/2 XXZ chain introduced in Section II B and having the anisotropy and the coupling given by Eqs. (5)-(6):

$$H^{(0)}_{\rm XXZ} \equiv \mathcal{P}H_{\rm BH}\mathcal{P} = -J\sum_i \Big(s_i^x s_{i+1}^x + s_i^y s_{i+1}^y - \frac{V}{J}s_i^z s_{i+1}^z\Big) \tag{34}$$

with $J = 2t\left(f+\frac{1}{2}\right)$ (constant terms have been omitted). The effective spin-1/2 operators are defined as

$$\begin{aligned} s_i^x &= \frac{1}{2\sqrt{f+\frac{1}{2}}}\mathcal{P}\left(b_i + b_i^\dagger\right)\mathcal{P},\\ s_i^y &= \frac{i}{2\sqrt{f+\frac{1}{2}}}\mathcal{P}\left(-b_i + b_i^\dagger\right)\mathcal{P},\\ s_i^z &= \mathcal{P}\left(b_i^\dagger b_i - f\right)\mathcal{P}; \end{aligned} \tag{35}$$

the boson number eigenstates at site i correspond to the eigenstates of s_i^z according to $|\bar{n}\rangle_i \leftrightarrow |\downarrow\rangle_i$, and $|\bar{n}+1\rangle_i \leftrightarrow |\uparrow\rangle_i$. Therefore, the result in Eq. (34) corresponds to the "naive" large-U limit for the BH model at half-integer filling discussed in Section II B, in which off-diagonal matrix elements of relevant operators (including the Hamiltonian itself) are set to zero from the very beginning.

Corrections to $H^{(0)}_{\rm XXZ}$ arising from virtual transitions involving states outside of $\mathcal{F}$ may be properly accounted for within GW procedure, allowing to get the effective spin-1/2 Hamiltonian to the next order in t/U. Summing over all virtual transitions outside of $\mathcal{F}$ induced by H_I, one finds

$$\begin{aligned} H^{(1)} \equiv \mathcal{P}[H_I,\mathbf{a_1}]\mathcal{P} = -t^2\sum_{j,\ell}\mathcal{P}\left(b_j^\dagger b_{j+1} + b_{j+1}^\dagger b_j\right)\times\\ \times(\mathbf{I}-\mathcal{P})\,(H_{\rm BH})^{-1}\,(\mathbf{I}-\mathcal{P})\left(b_\ell^\dagger b_{\ell+1} + b_{\ell+1}^\dagger b_\ell\right)\mathcal{P}. \end{aligned} \tag{36}$$

In particular, when computing $H^{(1)}$, one has to consider intermediate states with either one of the μ_j in Eq. (18) being equal to 2, or to -1 (all these states have energy $\sim U$, with respect to states in the subspace $\mathcal{F}$), or states with one of the μ_j equal to 2 (-1), and the other equal to -1 (2) (all these states have energy $\sim 2U$, with respect to states in the subspace $\mathcal{F}$). Thus, one eventually finds out that $H^{(1)}$ can be written as the sum of two terms: $H^{(1)} = H^{(1)}_{\rm diag} + H^{(1)}_{\rm offd}$, with $H^{(1)}_{\rm diag}$ being the part of $H^{(1)}$ having 1- and 2-nearest-neighbour spin terms, while $H^{(1)}_{\rm offd}$ contains 2-next-nearest-neighbour and 3-spin terms. Omitting constant terms, their expression are given by:

$$H^{(1)}_{\text{diag}} = -\frac{4(\bar{n}+1)t^2}{U}\sum_i s^z_i - \frac{t^2}{U}\left(3\bar{n}^2+6\bar{n}+4\right)\sum_i s^z_i s^z_{i+1} \tag{37}$$

$$H^{(1)}_{\text{offd}} = -\frac{t^2(\bar{n}+1)^2}{U}\sum_i \left(s^+_{i+1}s^-_{i-1}+s^-_{i+1}s^+_{i-1}\right) - \frac{2t^2(\bar{n}+1)}{U}\sum_i \left(s^+_{i+1}s^-_{i-1}+s^-_{i+1}s^+_{i-1}\right)s^z_i . \tag{38}$$

As we shall in the next Section, using a Luttinger liquid representation, $H^{(1)}$ may be recasted in the XXZ form with coupling and anisotropy coefficients depending on U.

IV. EFFECTIVE XXZ PARAMETERS VIA A LUTTINGER LIQUID REPRESENTATION

The effective spin Hamiltonian in Eq. (33) is not in the XXZ form: in this Section we show how the contribution coming from $H^{(1)}$ may be accounted for by a pertinent redefinition of the parameters of the spin-1/2 XXZ-Hamiltonian $H^{(0)}_{\text{XXZ}}$.

The first contribution to $H^{(1)}_{\text{diag}}$ in the right-hand side of Eq. (37) describes an effective magnetic field in the z direction[88], while the second term simply shifts the value of the XXZ anisotropy. At variance, the term $H^{(1)}_{\text{offd}}$ in Eq. (38) contains 3-spin, as well as non-nearest neighbour, couplings. To show how these terms can be accounted for via a redefinition of $H^{(0)}_{\text{XXZ}}$, it is most convenient to rewrite $H^{(1)}_{\text{offd}}$ in terms of the Jordan-Wigner (JW) fermions $a_j, a^\dagger_j$, as outlined in Appendix B. As a result, one writes $H^{(1)}_{\text{offd}}$ as a sum of a bilinear (H_2), plus a quartic (H_4) term, that is

$$H^{(1)}_{\text{offd}} \equiv H_2 + H_4 ,$$

with

$$H_2 = \frac{t^2(\bar{n}+1)}{U}\sum_i \left(a^\dagger_{i-1}a_{i+1}+a^\dagger_{i+1}a_{i-1}\right) \tag{39}$$

$$H_4 = \frac{2t^2(\bar{n}+1)^2}{U}\sum_i :a^\dagger_i a_i:\left(a^\dagger_{i-1}a_{i+1}+a^\dagger_{i+1}a_{i-1}\right) \tag{40}$$

Since H_2 is bilinear in the JW fermions, it merely modifies the single-fermion dispersion relation, yielding the quadratic Hamiltonian in the JW fermions reading

$$H^{(0)}_{\text{XXZ}} + H_2 = \sum_k \left\{ -2J\cos k + \frac{t^2(\bar{n}+1)}{U}\cos(2k) - B \right\} a^\dagger_k a_k , \tag{41}$$

with $B = 4(\bar{n}+1)t^2/U$. Setting $\epsilon(k) = -2J\cos k + \frac{t^2(\bar{n}+1)}{U}\cos(2k) - B$, one finds that the Fermi points, defined by $\epsilon(k_F)=0$, are given by

$$\cos k_F = \frac{U(\bar{n}+1)}{2J} - \sqrt{\left(\frac{U(\bar{n}+1)}{2J}\right)^2 + \bar{n}+2} . \tag{42}$$

Upon linearizing the dispersion relation around $\pm k_F$ and setting $k = k_F + p$, one gets

$$\epsilon(\pm k_F + p) \approx \pm J\sin k_F\left[1 - \frac{2J}{U(\bar{n}+1)}\cos k_F\right]p . \tag{43}$$

From Eq. (43) one sees that, since $\cos k_F \neq 0$, H_2 implies a nonzero effective magnetic field B_{eff}[88], as well as a redefinition of the Fermi velocity v_F. This yields a redefined coupling given by $B_{\text{eff}}/J_{\text{eff}} = -\cos k_F$. Since

$$B_{\text{eff}} = -J\cos k_F\left(1 - \frac{2J}{U}\cos k_F\right),$$

one obtains

$$J_{\text{eff}} = J\left(1 - \frac{2J}{U}\cos k_F\right). \tag{44}$$

The quartic term H_4 can be dealt with by noticing that, in the low-energy, long-wavelength limit, one can write

$$a^\dagger_{j-1}a_{j+1} + a^\dagger_{j+1}a_{j-1} \longrightarrow -\Big\{\rho_R(x_j)+\rho_L(x_j) - (-1)^j\left[\psi^\dagger_R(x_j)\psi_L(x_j)+\psi^\dagger_L(x_j)\psi_R(x_j)\right]\Big\} , \tag{45}$$

where the chiral fermion fields $\psi_R(x_j)$, $\psi_L(x_j)$ are defined from the long-wavelength expansion of a_j as (see Appendix B)

$$a_j \approx e^{ik_F x_j}\psi_R(x_j) + e^{-ik_F x_j}\psi_L(x_j), \tag{46}$$

with $x_j = aj$, and the chiral fermion densities given by $\rho_R(x_j) = \psi^\dagger_R(x_j)\psi_R(x_j)$ and $\rho_L(x_j) = \psi^\dagger_L(x_j)\psi_L(x_j)$. As a result, H_4 may be written as

$$H_4 = -\frac{4t^2(\bar{n}+1)^2}{U}\int_0^L dx\,\Big\{(\rho_R(x))^2 + (\rho_L(x))^2 + 4\rho_R(x)\rho_L(x)\Big\}. \tag{47}$$

Comparing Eq. (47) to Eq. (B13), one sees that H_4 takes the same form as the term $J\sum_j s^z_j s^z_{j+1}$ in the spin-1/2 XXZ Hamiltonian in Eq. (4).

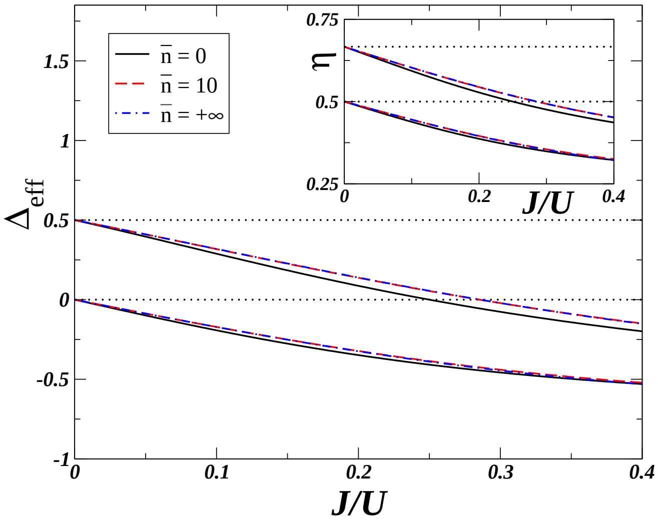

FIG. 1: $\Delta_{\rm eff}$ *vs.* J/U for different values of V/J and $\bar{n}$. The top (bottom) dotted line corresponds to the value of $\Delta_{\rm eff}$ for $U/J \to \infty$ and $V/J = 0.5$ ($V/J = 0$). The other lines are for $V/J = 0.5$ (top) and $V/J = 0$ (bottom), with $\bar{n} = 0$ (solid black lines), $\bar{n} = 10$ (dashed red lines) and $\bar{n} \to \infty$ (dot-dashed blue blue lines). Inset: same as in the main panel, but for η *vs.* J/U.

Collecting together all the above results allows to write an effective XXZ Hamiltonian, describing the BH model to the order $(t/U)^2$, as:

$$H^{\rm eff}_{\rm XXZ} = -J_{\rm eff} \sum_j \left(s^x_j s^x_{j+1} + s^y_j s^y_{j+1} - \Delta_{\rm eff} s^z_j s^z_{j+1} \right) , \tag{48}$$

with $J_{\rm eff}$ defined in Eq. (44) and

$$\Delta_{\rm eff} = \frac{\bar{\Delta}}{1 - \frac{2J}{U} \cos(k_F)} \tag{49}$$

with

$$\bar{\Delta} = \frac{V}{J} - \frac{t^2(3\bar{n}^2 + 6\bar{n} + 4)}{JU} - \frac{4t^2(\bar{n}+1)^2}{JU}. \tag{50}$$

Since $J_{\rm eff}$ acts just as an effective over-all scale of $H^{\rm eff}_{\rm XXZ}$, then $\Delta_{\rm eff}$ is the only parameter determining the behavior of spin-spin correlations in the XXZ model. Substituting Eq. (49) in Eq. (8) one gets

$$\eta = 1 - \frac{1}{\pi} \arccos \Delta_{\rm eff}, \tag{51}$$

which provides an explicit formula for the effective Luttinger parameter for the BH model at half-integer filling. In Fig. 1 we plot both $\Delta_{\rm eff}$ and η versus J/U, for different values of V/J and $\bar{n}$. One sees that $\bar{n} = 10$ and $\bar{n} \to \infty$ are almost indistinguishable, and that the limit of the quantum phase model for Josephson junction arrays ($\bar{n} \gg 1$) at offset charge $q = e$ is practically reached at $\bar{n} \sim 10$. Furthermore, one sees that the dependence of η upon $\bar{n}$ is rather small.

From Fig. 1 one also sees that $\Delta_{\rm eff}$ may be tuned by varying the ratio J/U: in particular $\Delta_{\rm eff}$ can be different from 0 even if $V = 0$ (as it is typical for alkali atoms). Fig. 1 also suggests the possibility of describing the whole phase diagram of the XXZ spin-1/2 chain using BH model for a single species of bosons with pertinently chosen parameters, see also Section VI[89].

Finally we notice that, since the sign of $\Delta_{\rm eff}$ may be changed by a pertinent choice of J/U and V, the Luttinger liquid effectively describing the XXZ-Hamiltonian may be repulsive or attractive. As noticed in the context of 1D Josephson junction arrays[72,73], the transition between the repulsive and the attractive side may be monitored by inserting a weak link (i.e., a nonmagnetic impurity[82]): it would be then interesting to analyze the effects of a weak link introduced in a bosonic system described by the BH Hamiltonian.

V. CORRELATION FUNCTIONS

The mapping between $H_{\rm BH}$ and $H^{\rm eff}_{\rm XXZ}$ derived in Section IV enables to select the ground-states on which to compute the pertinent vacuum expectation values. Indeed if $|\Phi_0\rangle$ is the ground-state of the BH Hamiltonian given in Eq. (3), and $|\Psi_0\rangle \equiv \mathbf{S}^\dagger |\Phi_0\rangle$ is the ground-state of $H_{\rm eff} = \mathbf{S}^\dagger H_{\rm BH} \mathbf{S}$, the GW approach requires

$$\begin{aligned} \langle \Phi_0 | \mathcal{O}_{\rm BH} \left[\{ b, b^\dagger \} \right] \Phi_0 \rangle &= \langle \Psi_0 | \mathbf{S}^\dagger \mathcal{O}_{\rm BH} \left[\{ b, b^\dagger \} \right] \mathbf{S} | \Psi_0 \rangle \\ &\equiv \langle \Psi_0 | \mathcal{O}_{\rm XXZ} \left[\{ s^a \} \right] | \Psi_0 \rangle, \end{aligned} \tag{52}$$

where $\mathcal{O}_{\rm BH} \left[\{ b, b^\dagger \} \right]$ ($\mathcal{O}_{\rm XXZ} \left[\{ s^a \} \right]$) denotes a generic BH (XXZ) operator. Of course, Eq. (52) is exact only if $\mathbf{S}$ is the exact solution of the GW equation (31): by computing it perturbatively at a given order, one recovers the correspondence between ground-state expectation values of BH and spin-1/2 operators at the chosen order.

In the rest of the paper, we will be interested in correlation functions of the following BH operators:

$$\mathcal{M}^z_{i,j} \equiv (n_i - f)(n_j - f) , \tag{53}$$

$$\mathcal{M}^\perp_{i,j} \equiv b^\dagger_i b_j . \tag{54}$$

Using the results of Appendix C one has $\mathbf{S}^\dagger \mathcal{M}^z_{i,j} \mathbf{S} = \mathcal{M}^z_{i,j} \left[1 + \mathcal{O}\left(\frac{t^2 \bar{n}^2}{U^2} \right) \right]$, so that

$$\langle \Phi_0 | (n_i - f)(n_j - f) | \Phi_0 \rangle = \langle \Psi_0 | s^z_i s^z_j | \Psi_0 \rangle + \mathcal{O}\left(\frac{t^2 \bar{n}^2}{U^2} \right). \tag{55}$$

More generally, if the operator $\mathcal{O}_{\rm BH}$ satisfies $(\mathbf{I} - \mathcal{P})\, \mathcal{O}_{\rm BH} \mathcal{P} = \mathcal{P} \mathcal{O}_{\rm BH} (\mathbf{I} - \mathcal{P}) = 0$, then $\langle \Phi_0 | \mathcal{O}_{\rm BH} | \Phi_0 \rangle \approx \langle \Psi_0 | \mathcal{O}_{\rm XXZ} | \Psi_0 \rangle$, with $\mathcal{O}_{\rm XXZ}$ obtained from $\mathcal{O}_{\rm BH}$ by substituting b_i, $b^\dagger_i$ and $n_i - f$ respectively with s^-_i, s^+_i and s^z_j. At variance, for $\mathcal{M}^\perp_{i,j}$ one obtains a more involved expression (see Appendix C for details):

$$\begin{aligned}\langle\Phi_0|b_i^\dagger b_j|\Phi_0\rangle \;\approx\; & (\bar{n}+1)\langle\Psi_0|s_i^- s_j^+|\Psi_0\rangle + \frac{t(\bar{n}+2)(\bar{n}+1)}{2U}\langle\Psi_0|[s_{i+1}^- + s_{i-1}^-]s_j^+ + \left[s_{j+1}^+ + s_{j-1}^+\right] s_i^-|\Psi_0\rangle \\ & + \frac{t\bar{n}(\bar{n}+1)}{2U}\langle\Psi_0|s_i^-[s_{j-1}^+ + s_{j+1}^+] + s_j^+\left[s_{i-1}^- + s_{i+1}^-\right]|\Psi_0\rangle + \delta_{|i-j|,1}\,\langle\Psi_0|\left(\frac{1}{2} - s_{i+1}^z\right)\left(\frac{1}{2} + s_i^z\right)|\Psi_0\rangle,\end{aligned}$$

where again we neglected contributions arising to $\mathcal{O}\left(\frac{t^2\bar{n}^2}{U^2}\right)$.

VI. RESULTS

In this Section we compare the numerical results obtained through DMRG for the correlation functions and the phase diagram of the BH model with the analytical predictions for the correlators from the effective Hamiltonian $H_{\mathrm{XXZ}}^{\mathrm{eff}}$ given by Eq. (48).

A. Correlation functions

Let us focus on the BH correlation functions. Since DMRG simulations are made on a finite number of sites L and for open boundary conditions, we may use Eqs. (13) and (14) yielding the zz and xy correlation functions of the XXZ model. We evaluate the values of the non-universal constants a, b, c defined in Eq. (17) both numerically, by DMRG simulations of the XXZ model, and using the analytical expressions presented in Refs. 44,45 and reported in Section II B. As confirmed in Ref. 43, the values of a, b, c obtained in the two ways are in excellent agreement. We show that the analytical expressions for the XXZ correlations are well confirmed by the numerical BH correlations also for small L (e.g., for $L = 30$) and for J/U relatively large (as large as ~ 0.5). It should be stressed that, at variance, the agreement is not very good by setting $\Delta_{\mathrm{eff}} = V/J$, i.e. by using the Hamiltonian $H_{\mathrm{XXZ}}^{(0)}$ obtained for $U \to \infty$ neglecting contributions arising from the GW procedure.

The correlators $\langle\Phi_0|\,(n_i - f)\,(n_j - f)\,|\Phi_0\rangle$ and $\langle\Phi_0|b_i^\dagger b_j|\Phi_0\rangle$ are evaluated from the corresponding XXZ quantities using respectively Eqs. (55) and (56). They are plotted as a function of $r = |i - j|$, with i and j such that[43] $i = (L - r + 1)/2$, $j = (L + r + 1)/2$ for odd r, and $i = (L - r)/2$, $j = (L + r)/2$ for even r (for instance, for $L = 100$ sites, $r = 1$ corresponds to $i = 50$, $j = 51$; $r = 2$ corresponds to $i = 49$, $j = 51$; $r = 3$ corresponds to $i = 49$, $j = 52$, and so on).

In Fig. 2 we plot our results for the density-density correlations $\langle(n_i - f)\,(n_j - f)\rangle$ for a typical set of values, i.e. for $U = 10t$, $V = 0.5t$, $f = 0.5$, corresponding to $J/U = 0.2$. Black dots (joint by a black line as a guide for eye) are the density-density correlations evaluated in the BH model, red squares (line) are the correlation functions $\langle s_i^z s_j^z\rangle$ in the ground-state of the XXZ chain with effective anisotropy Δ_{eff} given by (49) and the a, b, c constants numerically determined from DMRG simulations of the XXZ chain, while the green diamonds (line) correspond to a, b, c analytically determined from Eqs. (17) and (9)-(10)-(11). One sees that, up to numerical accuracy $\lesssim 10^{-5}$, the results obtained analytically for the XXZ effective model are in excellent agreement with results of the density-density BH model even at small distance. Blue triangles (line) display the XXZ Hamiltonian results in the $U \to \infty$ limit, with anisotropy $\Delta = V/J$ – one sees that the relative error is noticeably larger.

In Fig. 3 we plot the off-diagonal correlations $\langle b_i^\dagger b_j\rangle$ for the same set of values of the BH parameters (namely, $U = 10t$, $V = 0.5t$, $f = 0.5$, $L = 150$). The meaning of dots and lines is the same as in Fig. 2: also here one sees that the results obtained from the GW effective Hamiltonian $H_{\mathrm{XXZ}}^{\mathrm{eff}}$ are in much better agreement than the ones obtained using H_{XXZ} with $\Delta = V/J$, this happens even though J/U is as low as 0.2.

To quantify the agreement between BH and XXZ results, we consider the absolute value of the relative error done in evaluating a correlator $\mathcal{C}(r)$ as the ground-state average of the corresponding operators in the BH model $[\mathcal{C}_{\mathrm{BH}}(r)]$, and in the XXZ model $[\mathcal{C}_{\mathrm{XXZ}}(r)]$. More pre-

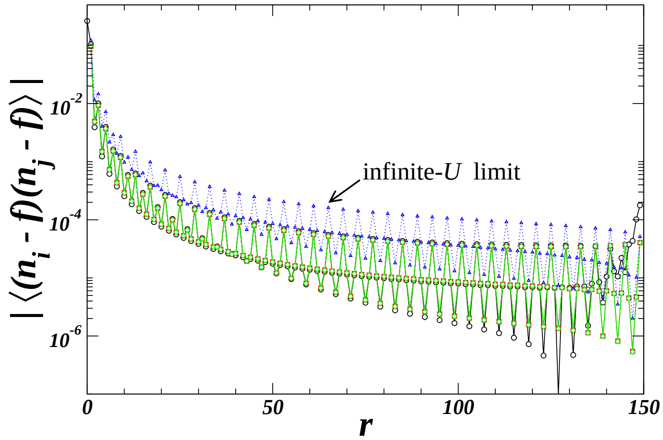

FIG. 2: Density-density correlations $|\langle(n_i - f)\,(n_j - f)\rangle|$ *vs.* $r = |i - j|$ for $U = 10t$, $V = 0.5t$ and $f = 0.5$, with number of sites $L = 150$. Black dots and line: BH results; red squares and line: XXZ result with a, b, c numerically determined; green diamonds and line: XXZ result with a, b, c analytically determined; blue triangles and dotted line: $U \to \infty$ XXZ result (indicated by the label "infinite-U limit" – see text fur further details).

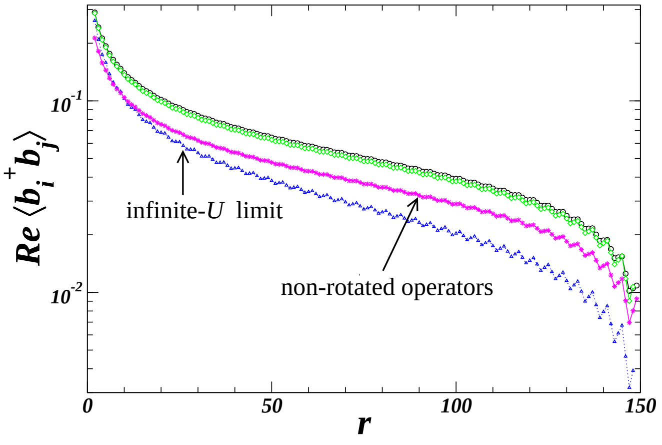

FIG. 3: Real part of $\langle b_i^\dagger b_j\rangle$ *vs.* $r = |i-j|$ for $U = 10t$, $V = 0.5t$, $f = 0.5$, $L = 150$. Magenta stars and line denote XXZ results with “non-rotated operators”.

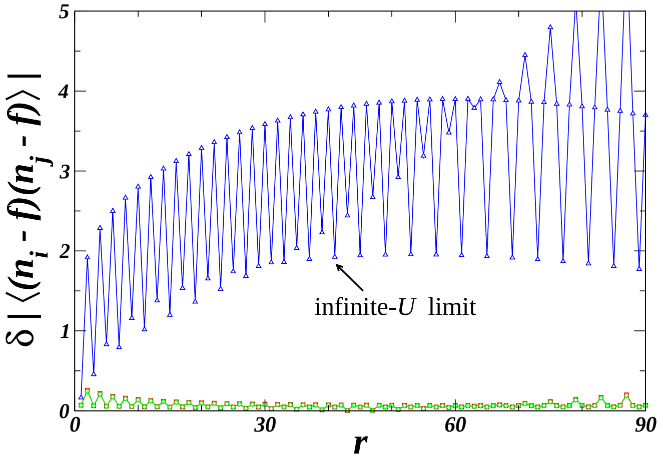

FIG. 4: Relative error of the correlation function $|\langle (n_i - f)\,(n_j - f)\rangle|$ *vs.* $r = |i-j|$ for the same parameters (and the same conventions for symbols and lines) of Fig. 1 – numerical XXZ red squares and analytical XXZ green diamonds for finite U almost coincide. The average value, with $r_{\rm max} = 3L/5$, is 0.06 ± 0.04 for the finite-U XXZ model and 2.9 ± 1.2 for the infinite-U XXZ model.

cisely, we define

$$\delta\mathcal{C}(r) = \left|\frac{\mathcal{C}_{\rm BH}(r) - \mathcal{C}_{\rm XXZ}(r)}{\mathcal{C}_{\rm BH}(r)}\right| \tag{56}$$

focusing on $\mathcal{C}_{zz}(r) \equiv |\langle (n_i - f)\,(n_j - f)\rangle|$ and $\mathcal{C}_{xy}(r) \equiv {\rm Re}\big[\langle b_i^\dagger b_j\rangle\big]$. To summarize the information on the relative error, we compute the average value $\delta_{\rm av}\mathcal{C}$ and the standard deviation of the relative error (56) for a distance $r = |i-j|$ between a minimum value $r_{\rm min} = 1$ (2) for zz (xy) correlations, and a maximum value $r_{\rm max} \sim 3L/5$.

The relative errors for the zz and xy correlation functions are plotted in Figs. 4-5: the error made using the GW $H^{\rm eff}_{\rm XXZ}$ is of the order of few percents (in agreement with $(J/U)^2 = 0.04$). At variance, the relative error made by using the XXZ model in the infinite-U limit without applying the GW procedure is much larger, although the value of J/U is not so large. Indeed, the error $\delta_{\rm av}$ is $\sim 300\%$ for the zz correlations and $\sim 40\%$ for the xy correlations (to be compared with $\sim 6\%$ and $\sim 3\%$ obtained from $H^{\rm eff}_{\rm XXZ}$). We checked that these results do not depend on the particular choice of $r_{\rm max}$: of course, when $r_{\rm max}$ is closer to L, the error is larger (especially for the density-density correlations) due to boundary effects. From the data of Figs. 4-5, one also sees that, at short distance, it is larger than that at intermediate distances (with r being few units it is $\lesssim 10\%$). As expected, it decreases at the center of the chain $r \sim L/2$, while, close to the end of the chain $r \sim L$, it increases. We also observe that finite-size effects are less visible for xy correlations.

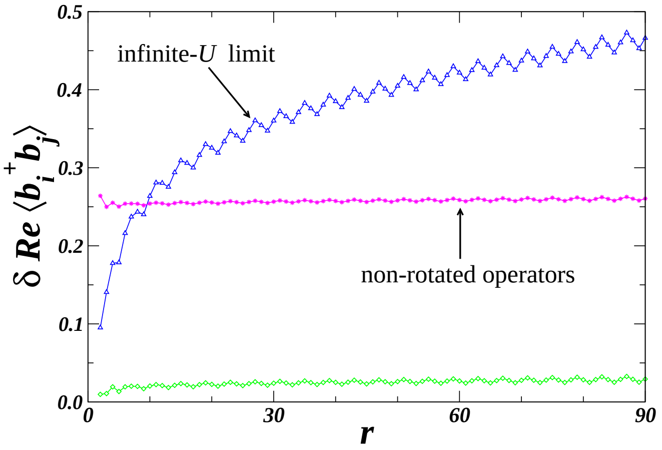

FIG. 5: Relative error of the real part of $\langle b_i^\dagger b_j\rangle$ *vs.* $r = |i-j|$ for the same parameters (and the same conventions for symbols and lines) of Fig. 2. The average values, with $r_{\rm max} = 3L/5$, are: 0.025 ± 0.004 (green diamonds - analytical XXZ results), 0.38 ± 0.08 (blue triangles - XXZ result in the infinite-U limit), 0.26 ± 0.03 (magenta stars - finite-U result with non-rotated operators).

The agreement between numerical and analytical results turns out to be stable also if one takes chains with smaller sizes, as it is apparent from Figs. 6-7, where we plot the zz and xy correlation functions for different sizes L. The corresponding errors are given in the following table:

L	$\delta^{(U)}_{\rm av}\mathcal{C}_{zz}$	$\delta^{(\infty)}_{\rm av}\mathcal{C}_{zz}$	$\delta^{(U)}_{\rm av}\mathcal{C}_{xy}$	$\delta^{(\infty)}_{\rm av}\mathcal{C}_{xy}$
30	0.12 ± 0.08	1.7 ± 0.9	0.04 ± 0.01	0.26 ± 0.07
50	0.10 ± 0.06	2.0 ± 1.0	0.04 ± 0.01	0.29 ± 0.08
80	0.09 ± 0.05	2.4 ± 1.0	0.04 ± 0.01	0.33 ± 0.08
100	0.08 ± 0.05	2.5 ± 1.1	0.04 ± 0.01	0.35 ± 0.08
150	0.07 ± 0.04	2.9 ± 1.2	0.04 ± 0.01	0.38 ± 0.08

where for simplicity $\delta^{(U)}_{\rm av}$ ($\delta^{(\infty)}_{\rm av}$) denotes the average error for the XXZ correlators at finite-U (infinite-U limit) with (without) the GW procedure. We see that, for the density-density zz correlations, the average error increases when the size L decreases.

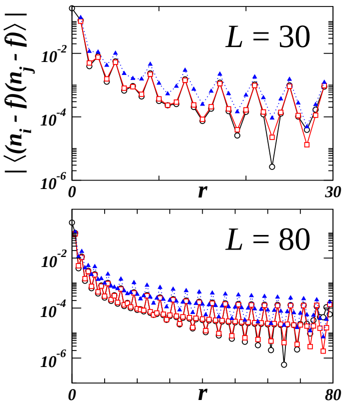

FIG. 6: In each panel we plot $|\langle(n_i - f)\,(n_j - f)\rangle|$ *vs.* $r = |i-j|$ for different sizes: $L = 30, 50, 80, 100$ ($U = 10t$, $V = 0.5t$, $f = 0.5$). The blue data (filled triangles) denote the infinite-U XXZ results.

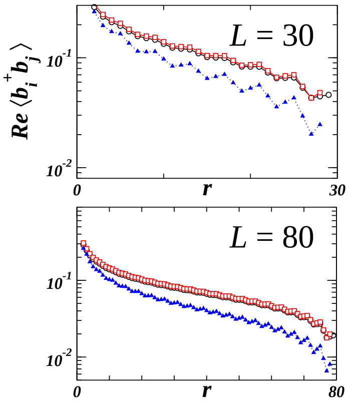

FIG. 7: Real part of $\langle\hat{b}_i^\dagger \hat{b}_j\rangle$ *vs.* $r = |i-j|$ for the sizes and the parameters of Fig. 6.

In Figs. 3 and 5 we also plotted (magenta stars and lines) the results obtained according to Eq. (52), where we took $\mathcal{O}_{\rm XXZ} = \mathcal{O}_{\rm BH}$ and not $\mathcal{O}_{\rm XXZ} = \mathbf{S}^\dagger \mathcal{O}_{\rm BH} \mathbf{S}$. Indeed, as stressed in Ref. 90, solving the equation for $\mathbf{S}$ amounts to perturbatively find a transformation enabling to block-diagonalize $H_{\rm BH}$. The ground-state of $H_{\rm BH}$ changes accordingly: if one wants to compute expectation values of certain operators in the BH model, one has to rotate the chosen operator according the $\mathbf{S}$ transformation - in other words, physical quantities in the effective theory are not simply the expectation values of the operators in the projected subspace: this guarantees the unitarity of the procedure. An example is already provided in Ref. 50 for the computation of the staggered magnetization in the 2D Fermi-Hubbard model with large-U effective spin models. In Appendix C we give details on the the explicit computation of the GW rotation for the operators $b_i^\dagger b_j$ and $(n_i - f)\,(n_j - f)$. We remark that, while for density-density correlation functions (zz correlations in the XXZ model) magenta stars coincide with the black circles, this is not the case for $\langle b_i^\dagger b_j\rangle$ (xy planar correlations in the XXZ model).

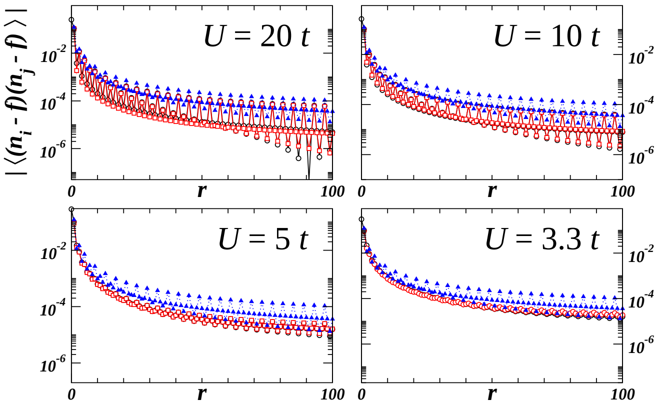

FIG. 8: Density-density correlations $|\langle(n_i - f)\,(n_j - f)\rangle|$ *vs.* $r = |i-j|$ for different values of $U/t = 20, 10, 5, 3.3$, corresponding, respectively, to $J/U = 0.1, 0.2, 0.4, 0.6$ (with $V = 0.5t$, $f = 0.5$, $L = 150$). The infinite-U result in each plot is the top blue line (triangles), while the other two - almost coinciding - lines are the numerical BH (black circles) and XXZ (red squares) results.

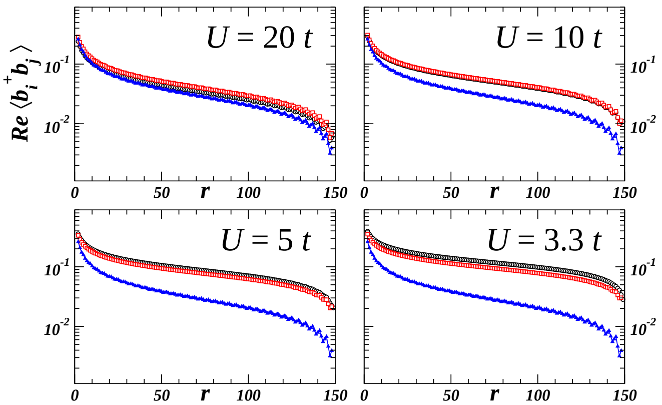

FIG. 9: Real part of $\langle\hat{b}_i^\dagger \hat{b}_j\rangle$ *vs.* $r = |i-j|$ for the same parameters (and the same conventions for symbols and lines) of Fig. 8.

In Figs. 8-9 we plot the zz and xy correlation functions for different values of U: in these plots the ratio J/U ranges from 0.1 to 0.6. As expected, one sees that for $J/U = 0.1$ the relative error made by the infinite-U results is not very large ($\sim 10\%$ for $\langle b_i^\dagger b_j\rangle$ correlations), but, as soon as $J/U \gtrsim 0.2$, it is already well visible. The relative error made by using the effective $H^{\rm eff}_{\rm XXZ}$ turns out rather small even for $J/U = 0.6$, where the relative error on density-density correlations is only $\approx 7\%$, while for $\langle b_i^\dagger b_j\rangle$ correlations it is $\approx 15\%$[91].

B. Antiferromagnet and domain ferromagnet in the 1D Bose-Hubbard model

The XXZ model is gapless and critical for $-1 \leq \Delta \leq 1$, antiferromagnetic for $\Delta > 1$ and ferromagnetic for $\Delta < -1$: in the latter ferromagnetic phase, all the spins are aligned. However, the BH at half-integer filling maps into the effective XXZ chain (48) supplemented by the condition that the total spin is vanishing: therefore we expect that, in the BH model at $\Delta_{\text{eff}} < -1$, domain walls form separating regions with "up" spins (i.e, with $f+1/2$ particles per site) and regions with "down" spins (i.e., with $f-1/2$ particles per site). At variance, at $\Delta_{\text{eff}} > 1$ the staggered magnetization becomes non vanishing: in the bosonic BH language the antiferromagnetic state corresponds to the "charge-checkerboard ordered state" $|f+1/2, f-1/2, f+1/2, f-1/2, \cdots\rangle$.

This shows that, consistently with the XXZ representation of the BH model at half-integer filling, at finite U one can realize the transition between the spin-liquid and the Néel-Ising antiferromagnetic phase of the XXZ model (superfluid-to-charge density wave phase transition of the BH model), as well as the transition between the spin-liquid and the domain ferromagnetic Ising phase of the XXZ model (superfluid-to-domain Mott-insulating phase transition of the BH model)[89]. Since the former transition sets in at $\Delta_{\text{eff}} = 1$ and the latter one at $\Delta_{\text{eff}} = -1$, using Eq. (49) for Δ_{eff} allows to determine the corresponding phase boundaries in terms of the parameters of the BH Hamiltonian.

A complete discussion of the phase diagram of the BH chain in presence of nearest-neighbour interactions is provided in Ref. 63: here we just focus on the half-integer BH chain with parameters chosen so as to lie close to $\Delta_{\text{eff}} = \pm 1$, in order to show that the effective XXZ representation given in this paper also provides a good description of these transitions.

For the spin liquid-ferromagnetic transition, we studied the BH chain with open boundary conditions varying V (similar results are obtained varying t) and we plot in Fig. 10 the expectation value of $(n_i - f)$ as a function of the position i along the chain. We observe that, as a consequence of the open boundary conditions, a magnetic field proportional to V on the two boundaries (i.e., at $i = 1$ and $i = L$) appears, whose effect close to the boundaries is clearly visible in the figure. Computing the quantity $\mathcal{N} = \sum_r (-1)^{i-j} \langle (n_i - f)(n_j - f) \rangle$, one sees that it significantly increases around a critical value Δ_{eff}^{AF}. From the numerical data for the BH model shown in Fig. 10 one may estimate $\Delta_{\text{eff}}^{AF} \sim 1.05$, in good agreement with the analytical value $\Delta_{\text{eff}}^{AF} = 1$[95]. We notice that a better estimate of Δ_{eff}^{AF} could be performed by adding a magnetic field in the boundaries to compensate the boundary magnetic fields arising from the open boundary conditions.

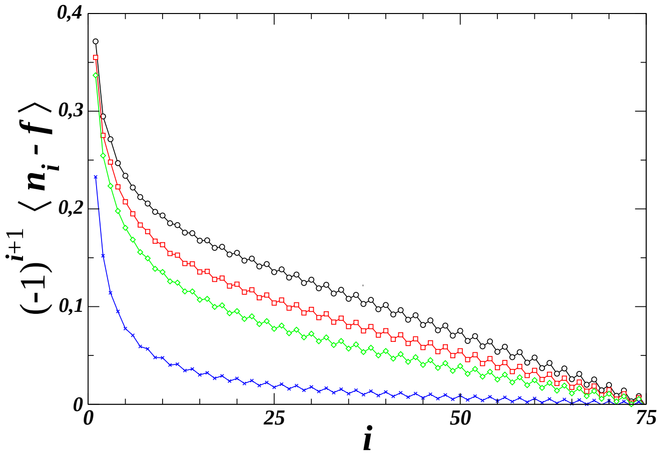

FIG. 10: Plot of $(-1)^{i+1}\langle n_i - f\rangle$ *vs.* i numerically computed in the BH chain for $U = 10t$, $f = 0.5$ and $L = 150$ for different values of V: from top to bottom $V/t = 3.3$ (black circles), $V/t = 3.1$ (red squares), $V/t = 2.9$ (green diamonds) and $V/t = 2$ (blue stars) corresponding, respectively, to $\Delta_{\text{eff}} = 1.09, 1.00, 0.91, 0.52$.

Regarding the domain ferromagnet-superfluid transition, we performed numerical simulations on the BH model with parameters chosen such that Δ_{eff} is close to -1 (see Figs. 11-12). In Fig. 11 we plot $\langle n_i - f \rangle$ as a function of the position i: one sees that the expectation value of the spin is constant and it changes sign close to the edges of the chain in order to satisfy the constraint on the number conservation. For this reason we then plot the modulus of the same quantity in Fig. 12: since the average of the s_i^z expectation values is of course zero, to determine the transition point from BH numerical data we consider the averaged quantity $\sum_{i=1}^{L} |\langle n_i - f \rangle|$ (e.g., for the different values of V shown in Fig. 12, such quantity is reported in the caption). From these data one can estimate that the domain ferromagnet is occurring at $\Delta_{\text{eff}}^{F} \sim -1.02$, with an error of few percent with respect to the analytical result $\Delta_{\text{eff}}^{F} = -1$[95]. Notice that the error made by using H_{XXZ} with $\Delta = V/J$ in the infinite-U limit is $\approx 20\%$: as expected, the errors made in using the infinite-U results are generally smaller when one deals with global quantities.

VII. CONCLUDING REMARKS

In this paper we studied an XXZ representation of the Bose-Hubbard chain at half-integer filling for finite on-site interaction energy U. The effective XXZ model is obtained in two steps: first, we used a similarity renormalization group procedure amounting to solve perturbatively up to the order $(t/U)^2$ the exact equation for the operator block-diagonalizing the Bose-Hubbard model. The resulting spin-1/2 effective Hamiltonian is then recasted as a XXZ spin-1/2 Hamiltonian with pertinently redefined coupling and anisotropy parameters.

We use this mapping to provide analytical estimates of the correlation functions of the Bose-Hubbard model at half-integer filling and finite U. We then compared

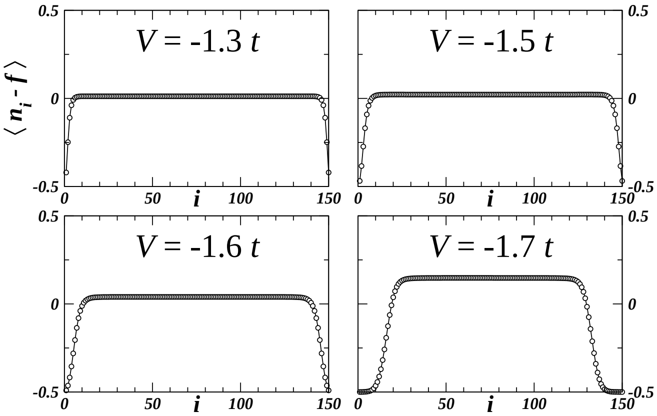

FIG. 11: Plot of $\langle n_i - f\rangle$ *vs.* i numerically computed in the BH chain for $U = 10t$, $f = 0.5$ and $L = 150$ for different values of V: $V/t = -1.3, -1.5, -1.6, -1.7$, corresponding, respectively, to $\Delta_{\text{eff}} = -0.91, -1.00, -1.04, -1.08$.

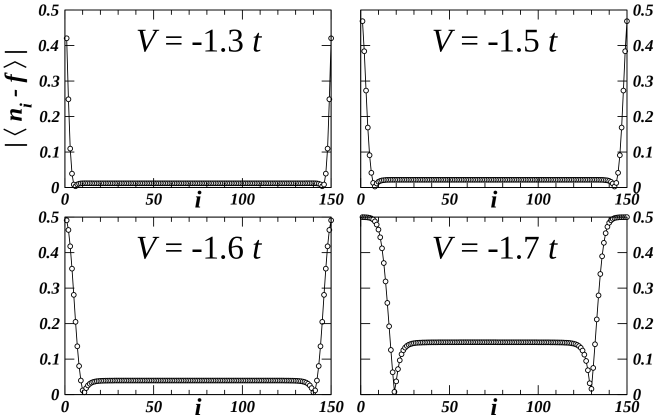

FIG. 12: Plot of the modulus of $\langle n_i - f\rangle$ *vs.* i computed in the BH chain for the same parameters of Fig. 11: $V/t = -1.3, -1.5, -1.6, -1.7$. The corresponding averages are $\approx 0.02, 0.04, 0.06, 0.21$.

these analytical results with the outcomes of the numerical DMRG evaluation of the Bose-Hubbard correlation functions. We found that the agreement is very good, also for J/U rather large (~ 0.5) and for small number of sizes ($L \sim 30$). Such a good agreement is not achieved - even for J/U relatively small (~ 0.1) - if one uses the XXZ Hamiltonian $H^{(0)}_{\text{XXZ}}$ with $J = 2t(f + 1/2)$ and $\Delta = V/J$ corresponding to the infinite-coupling limit of the Bose-Hubbard model. The transitions predicted at $\Delta_{\text{eff}} = \pm 1$ for the XXZ chain are as well compared with Bose-Hubbard results, and a good agreement is found.

Since the BH model at half-integer filing is not integrable or exactly solvable, it is quite valuable to have analytical estimates for its correlation functions. Besides its mathematical interest, we stress out that our results can be viewed from a two-fold point of view: on one side, we use known results from the (integrable) XXZ model to construct with high accuracy correlation functions of the Bose-Hubbard model. On the other side, the Bose-Hubbard chain at half-filling and at finite U may be seen as a quantum simulator of the XXZ chain.

In our approach, the effect of an harmonic trap results in a locally varying magnetic field: we feel that it would be interesting to compare the results stemming from an XXZ-based approach with the ones known in literature for hard- and soft-core bosons in harmonic traps in the scaling limit[92]. In this paper we focused on the half-integer filling Bose-Hubbard model, but deviations from such filling could be easily accounted with the introduction of a magnetic field. We stress that the similarity Hamiltonian renormalization procedure could also be applied to bosonic ladders[93] and at integer filling, where a spin-1 model is found in the infinite-U limit.

The large-V effects of edge magnetic field could also be studied, following the results known for the XXZ chain[94]: we observe that, for open boundary conditions and finite V, two boundary magnetic field terms $-B_b(s^z_1 + s^z_L)$, with $B_b \propto V$, emerge in the XXZ effective Hamiltonian[96]. Since a magnetic field at the edge induces corrections to the average value of s^z_i decreasing as a power law[94], these corrections are not only expected, but could be also worth the effort of future investigation.

Acknowledgments

We would like to thank F. Becca, L. Campos-Venuti, F. Essler, A. Ferraz, V. Korepin, F. Minardi, M. Müller, G. Santoro and A. Smerzi for very useful discussions. A.T. acknowledges kind hospitality from IIP-UFRN (Natal), where part of this work was performed. D.R. acknowledges financial support from EU through the project SOLID.

Appendix A: Perturbative solution of the GW equation

In this Appendix we show how use Eq. (30) to determine $\mathbf{a}$ to *first order* in H_I, that is $\mathbf{a_1}$. To this order, one gets

$$\mathcal{P}\left\{H_I + [H_0, \mathbf{a_1}]\right\}(\mathbf{I} - \mathcal{P}) = 0, \tag{A1}$$

which may be solved by setting

$$\begin{aligned}
&\mathcal{P}\mathbf{a_1}\,(\mathbf{I} - \mathcal{P}) = \\
&\mathcal{P}H_I\,(\mathbf{I} - \mathcal{P})\Big\{ -\mathcal{P}H_0\mathcal{P} + (\mathbf{I} - \mathcal{P})\,H_0\,(\mathbf{I} - \mathcal{P})\Big\}^{-1} \\
&+[\mathcal{P}H_0\mathcal{P}, \mathcal{P}\mathbf{a_1}\,(\mathbf{I} - \mathcal{P})] \\
&\times\Big\{ -\mathcal{P}H_0\mathcal{P} + (\mathbf{I} - \mathcal{P})\,H_0\,(\mathbf{I} - \mathcal{P})\Big\}^{-1}.
\end{aligned} \tag{A2}$$

Up to term that are second order in $t\bar{n}/U$, we may make the approximation $\mathcal{P}H_0\mathcal{P} \approx \mathcal{E}_0[\bar{n}]\mathbf{I}$, with $\mathcal{E}_0[\bar{n}] = L\left\{\frac{U}{2}\bar{n}(\bar{n} - 1) + V\bar{n}^2\right\}$, which implies

$[\mathcal{P}H_0\mathcal{P}, \mathcal{P}\mathbf{a}\,(\mathbf{I}-\mathcal{P})] = 0$. As a result, we get

$$\begin{aligned} &\mathcal{P}\mathbf{a_1}\,(\mathbf{I}-\mathcal{P}) = \mathcal{P}H_I\,(\mathbf{I}-\mathcal{P}) \\ &\times\{-\mathcal{P}H_0\mathcal{P} + (\mathbf{I}-\mathcal{P})\,H_0\,(\mathbf{I}-\mathcal{P})\}^{-1}. \end{aligned} \tag{A3}$$

Using the fact that $\mathbf{a}$ is antihermitean, from Eq. (A3) one obtains

$$\begin{aligned} &\mathbf{a_1} = \mathcal{P}H_I\,(\mathbf{I}-\mathcal{P}) \\ &\times\Big\{-\mathcal{P}H_0\mathcal{P} + (\mathbf{I}-\mathcal{P})\,H_0\,(\mathbf{I}-\mathcal{P})\Big\}^{-1} - \\ &\Big\{-\mathcal{P}H_0\mathcal{P} + (\mathbf{I}-\mathcal{P})\,H_0\,(\mathbf{I}-\mathcal{P})\Big\}^{-1} \\ &\times(\mathbf{I}-\mathcal{P})\,H_I\mathcal{P}. \end{aligned} \tag{A4}$$

Appendix B: Jordan-Wigner fermion representation for the spin-1/2 XXZ spin chain

In this Appendix we review the basic ingredients for fermionizing the spin-1/2 XXZ chain by means of JW fermions, which is used in the main text derive the effective parameters to $H^{\mathrm{eff}}_{\mathrm{XXZ}}$ (see Section IV).

We start from the spin-1/2 XXZ Hamiltonian with periodic boundary conditions:

$$H_{\mathrm{XXZ}} = \sum_{i=1}^{L} -J\left(s_i^+ s_{i+1}^- + s_{i+1}^+ s_i^- - \Delta s_i^z s_{i+1}^z\right) - B s_i^z, \tag{B1}$$

where $s^\alpha_{L+1} \equiv s^\alpha_1$. The JW-fermion representation is realized in terms of lattice complex fermions $a_i, a_i^\dagger$,

$$s_i^+ = a_j^\dagger e^{i\pi\sum_{r=1}^{i-1} a_r^\dagger a_r}, \quad s_i^z = a_j^\dagger a_i - \frac{1}{2}. \tag{B2}$$

The first step is to fermionize the $s^+\,s^-$ term in the standard XXZ spin-1/2 Hamiltonian plus a possible magnetic field contribution: this yields $H_{\mathrm{XXZ}} \to H_2^{(0)}$ with

$$H_2^{(0)} \equiv \sum_{i=1}^{L} -J\left(a_i^\dagger a_{i+1} + a_{i+1}^\dagger a_i\right) - B\left(a_i^\dagger a_i - \frac{1}{2}\right). \tag{B3}$$

Defining the Fourier modes a_k as

$$a_k = \frac{1}{\sqrt{L}}\sum_{j=1}^{L} e^{ikj} a_j, \tag{B4}$$

one gets

$$H_2^{(0)} = \sum_k \epsilon_0(k) a_k^\dagger a_k \tag{B5}$$

with $\epsilon_0(k) = -2J\cos k - B$. Since the effective XXZ spin-1/2 Hamiltonian we derive in this paper is the effective description of a BH Hamiltonian at fixed filling in the canonical ensemble, the z-component of the total spin is set to 0 and the magnetic field term does not provide any contribution to the total Hamiltonian. Accordingly, we may set $B = 0$ from the beginning. This implies that the Fermi momenta are given by $\pm k_F = \pm\frac{\pi}{2a}$, where a is the lattice constant. As a consequence, the effective low-energy, long-wavelength Hamiltonian may be obtained by expanding the lattice fermion fields around the Fermi points $\pm k_F = \pm\frac{\pi}{2}$, as

$$a_j \approx \sqrt{a}\,\left\{e^{ik_F j}\psi_R(x_j) + e^{-ik_F j}\psi_L(x_j)\right\}, \tag{B6}$$

with

$$\begin{aligned} \psi_R(x_j) &= \frac{1}{\sqrt{L}}\sum_{|p|\le\Lambda} e^{ipx_j} a_{k_F+p}, \\ \psi_L(x_j) &= \frac{1}{\sqrt{L}}\sum_{|p|\le\Lambda} e^{ipx_j} a_{-k_F+p}, \end{aligned} \tag{B7}$$

x_j being equal to aj, while Λ is a pertinent cutoff in momentum space. Accordingly, the low-energy, long-wavelength quadratic part of the fermionized XXZ Hamiltonian will be given by

$$H_2^{(0)} \to iv_F \int_0^L dx\,\left\{\psi_L^\dagger(x)\frac{\partial\psi_L(x)}{\partial x} - \psi_R^\dagger(x)\frac{\partial\psi_R(x)}{\partial x}\right\}, \tag{B8}$$

with the Fermi velocity $v_F = 2aJ$. Moreover, since the ground-state $|\mathrm{G}\rangle$ of $H_2^{(0)}$ is defined by

$$|\mathrm{G}\rangle = \prod_{\epsilon_0(k)<0} a_k^\dagger|0\rangle, \tag{B9}$$

one gets that

$$\left(a_j^\dagger a_j - \frac{1}{2}\right) =: a_j^\dagger a_j :, \tag{B10}$$

where the colons denote normal ordering with respect to $|\mathrm{G}\rangle$. Accordingly, one may rewrite the “Ising“ contribution to the spin-1/2 XXZ Hamiltonian as

$$H_{\mathrm{Ising}} \equiv J\Delta\sum_{i=1}^{L-1} s_i^z s_{i+1}^z \longrightarrow J\Delta\sum_{i=1}^{L-1} :a_j^\dagger a_j: :a_{j+1}^\dagger a_{j+1}: . \tag{B11}$$

Resorting to continuum chiral fermion operators, from Eq. (B7) one obtains

$$\begin{aligned} :a_j^\dagger a_j: \;=\; & :\psi_R^\dagger(x_j)\psi_R(x_j): + :\psi_L^\dagger(x_j)\psi_L(x_j): \\ & +(-1)^j\left\{\psi_R^\dagger(x_j)\psi_L(x_j) + \psi_L^\dagger(x_j)\psi_R(x_j)\right\}. \end{aligned}$$

Setting

$$\begin{aligned} :a_j^\dagger a_j: \;\equiv\; & \rho_R(x_j) + \rho_L(x_j) \\ & +(-1)^j\left\{\psi_R^\dagger(x_j)\psi_L(x_j) + \psi_L^\dagger(x_j)\psi_R(x_j)\right\} \end{aligned} \tag{B12}$$

and summing over j one eventually gets

$$\begin{aligned} H_{\mathrm{Ising}} \;\to\; & J\Delta a\int_0^L dx_j\,\{(\rho_R(x_j))^2 + (\rho_L(x_j))^2 \\ & +4\rho_R(x_j)\rho_L(x_j)\} + H_{\mathrm{Umklapp}}. \end{aligned} \tag{B13}$$

The term H_{Umklapp} in Eq. (B13) arises from two-fermion scattering processes in which the total momentum exchanged by the particles is $\sim 4k_F = \frac{2\pi}{a}$. A systematic analysis of such a term may be provided within the framework of a Luttinger liquid theory, obtained by bosonization of JW fermions[29]. As our work is mainly concerned with the correspondence between the BH and the XXZ Hamiltonian, here we just point out that the Umklapp term may be either irrelevant, or relevant, according to whether $\Delta < 1/2$, or $\Delta > 1/2$. As soon as it becomes relevant, it triggers the phase transition between the spin liquid and the antiferromagnetic Neél phase of the XXZ model which, as we discussed in the main text, corresponds to the transition between the superfluid and the charge density wave phases of the BH model.

Appendix C: GW transformation of operators

An advantage of the GW procedure is that it may be easily applied to single-boson operators: in particular, we are interested in the average values of the operators $\mathcal{M}^{\perp}_{i,j}$ and $\mathcal{M}^{z}_{i,j}$ defined in Eqs. (53) and (54). Since $\mathbf{a_1}$ is fully off-diagonal and $\mathcal{P}\mathcal{M}^{z}_{i,j}\,(\mathbf{I}-\mathcal{P}) = 0$, if one approximates $\mathbf{T}$ with $\mathbf{a_1}$, one obtains $\mathbf{S}^\dagger\mathcal{M}^{z}_{i,j}\mathbf{S} = \mathcal{M}^{z}_{i,j}$. Instead, acting onto $\mathcal{M}^{\perp}_{i,j}$ gives raise to a more complicated expression: expressing the final result in terms of spin-1/2 variables, one obtains

$$\begin{aligned}
\mathcal{P}\mathbf{S}^\dagger\mathcal{M}^{\perp}_{i,j}\mathbf{S}\mathcal{P} \;\approx\;& \delta_{|i-j|,1}\,\frac{t\bar{n}(\bar{n}+2)}{U}\left(\frac{1}{2}-s^z_{i+1}\right)\left(\frac{1}{2}+s^z_i\right) \\
&+\;\frac{t(\bar{n}+2)(\bar{n}+1)}{U}\left\{s^-_{i+1}s^+_j\left(\frac{1}{2}+s^z_i\right)+s^-_{i-1}s^+_j\left(\frac{1}{2}+s^z_i\right)+s^-_i s^+_{j+1}\left(\frac{1}{2}+s^z_j\right)+s^-_i s^+_{j-1}\left(\frac{1}{2}+s^z_j\right)\right\} \\
&+\;\frac{t(\bar{n}+2)(\bar{n}+1)}{2U}\left\{s^-_i s^+_{j-1}\left(\frac{1}{2}-s^z_i\right)+s^-_i s^+_{j+1}\left(\frac{1}{2}-s^z_i\right)+s^-_{i-1}s^+_j\left(\frac{1}{2}-s^z_j\right)+s^-_{i+1}s^+_j\left(\frac{1}{2}-s^z_j\right)\right\}.
\end{aligned} \tag{C1}$$

We observe that due to the constraint on the fixed total particle number N, the total magnetization in any of the physical states of $H_{\text{eff}} = H^{(0)}_{\text{XXZ}} + H^{(1)}_{\text{diag}} + H^{(1)}_{\text{offd}}$ is zero: since H_{eff} contains no terms breaking the parity symmetry ($s^\alpha_i \to -s^\alpha_i$), its ground-state $|\Psi_0\rangle$ is nondegenerate and, thus, it must be parity invariant. As a consequence, the average of any product of three spin-1/2 operators must necessarily give 0, greatly simplifying the calculation of the ground-state average of the operator.

Using this result one can obtain a simplified expression for $\langle\Phi_0|\mathcal{M}^{\perp}_{i,j}|\Phi_0\rangle$ at $\mathcal{O}\left(\frac{t^2\bar{n}^2}{U^2}\right)$: one has

$$\begin{aligned}
&\langle\Phi_0|\mathcal{M}^{\perp}_{i,j}|\Phi_0\rangle \approx \delta_{|i-j|,1}\,\langle\Psi_0|\left(\frac{1}{2}-s^z_{i+1}\right)\left(\frac{1}{2}+s^z_i\right)|\Psi_0\rangle \\
&+\frac{t(\bar{n}+2)(\bar{n}+1)}{U}\langle\Psi_0|\left\{s^-_{i+1}s^+_j\left(\frac{1}{2}+s^z_i\right)+s^-_{i-1}s^+_j\left(\frac{1}{2}+s^z_i\right)+s^-_i s^+_{j+1}\left(\frac{1}{2}+s^z_j\right)+s^-_i s^+_{j-1}\left(\frac{1}{2}+s^z_j\right)\right\}\mathcal{P}|\Psi_0\rangle \\
&+\frac{t\bar{n}(\bar{n}+1)}{U}\langle\Psi_0|\mathcal{P}\left\{s^-_i s^+_{j-1}\left(\frac{1}{2}-s^z_i\right)+s^-_i s^+_{j+1}\left(\frac{1}{2}-s^z_i\right)++s^-_{i-1}s^+_j\left(\frac{1}{2}-s^z_j\right)+s^-_{i+1}s^+_j\left(\frac{1}{2}-s^z_j\right)\right\}\mathcal{P}|\Psi_0\rangle
\end{aligned} \tag{C2}$$

Since any product of three spin-1/2 operators must necessarily give 0, then Eq. (C2) gives Eq. (56) reported in the main text.

---

[1] S. Blundell, *Magnetism in condensed matter* (Oxford, Oxford University Press, 2001).

[2] *Introduction to frustrated magnetism: materials, experiments, theory*, eds. C. Lacroix, P. Mendels, and F. Mila (Heidelberg, Springer, 2011).

[3] G.B. Jo, Y.R. Lee, J.H. Choi, C.A. Christensen, T.H. Kim, J.H. Thywissen, D.E. Pritchard, and W. Ketterle, Science **325**, 1521 (2009).

[4] K. Kim, M.S. Chang, S. Korenblit, R. Islam, E.E. Edwards, J.K. Freericks, G.D. Lin, L.-M. Duan, and C. Monroe, Nature **465**, 590 (2010).
[5] S. Fölling, S. Trotzky, P. Cheinet, M. Feld, R. Saers, A. Widera, T. Müller, and I. Bloch, Nature **448**, 1029 (2007).
[6] A. Eckardt, C. Weiss, and M. Holthaus, Phys. Rev. Lett. **95**, 260404 (2005).
[7] J. Struck, C. Olschlager, R. Le Targat, P. Soltan-Panahi, A. Eckardt, M. Lewenstein, P. Windpassinger, and K. Sengstock, Science **333**, 996 (2011).
[8] L.-M. Duan, E. Demler, and M.D. Lukin, Phys. Rev. Lett. **91**, 090402 (2003).
[9] G. Thalhammer, G. Barontini, L. De Sarlo, J. Catani, F. Minardi, and M. Inguscio, Phys. Rev. Lett. **100**, 210402 (2008).
[10] A. B. Kuklov and B.V. Svistunov, Phys. Rev. Lett. **90**, 100401 (2003).
[11] I. Bloch, J. Dalibard, and W. Zwerger, Rev. Mod. Phys. **80**, 885 (2008).
[12] D. Jaksch, C. Bruder, J.I. Cirac, C.W. Gardiner, and P. Zoller, Phys. Rev. Lett. **81**, 3108 (1998).
[13] J.J. García-Ripoll, M.A. Martin-Delgado, and J.I. Cirac, Phys. Rev. Lett. **93**, 250405 (2004).
[14] S. Sachdev, K. Sengupta, and S.M. Girvin, Phys. Rev. B **66**, 075128 (2002).
[15] B.K. Chakrabarti, A. Dutta, and P. Sen, *Quantum Ising phases and transitions in transverse Ising models* (Berlin, Springer-Verlag, 1996).
[16] J. Simon, W.S. Bakr, R.C. Ma, M.E. Tai, P.M. Preiss, and M. Greiner, Nature **472**, 307 (2011).
[17] M.P.A. Fisher, P.B. Weichman, G. Grinstein, and D.S. Fisher, Phys. Rev. B **40**, 546 (1989).
[18] M. Greiner, O. Mandel, T. Esslinger, T.W. Hansch, and I. Bloch, Nature **415**, 39 (2002).
[19] C. Bruder, R. Fazio, and G. Schón, Ann. Phys. **14**, 566 (2005).
[20] I. Bloch, Nature **453**, 1016 (2008).
[21] O. Morsch and M.K. Oberthaler, Rev. Mod. Phys. **78**, 179 (2006).
[22] A. Polkovnikov, K. Sengupta, A. Silva, and M. Vengalattore, Rev. Mod. Phys. **83**, 863 (2011).
[23] T. Matsubara and H. Matsuda, Prog. Theor. Phys. **16**, 416 (1956); *ibid.* **16**, 569 (1956); *ibid.* **17**, 19 (1957).
[24] R.A. Aziz, V.P.S. Nain, J.S. Carley, W.L. Taylor, and G.T McConville, J. Chem. Phys. **70**, 4330 (1979).
[25] D.C. Mattis, *The theory of magnetism I: Statics and dynamics* (Berlin, Springer-Verlag, 1981).
[26] H.A. Bethe, Z. Physik **71**, 205 (1931).
[27] M. Takahashi, *Thermodynamics of one-dimensional solvable models* (Cambridge, Cambridge University Press, 2005).
[28] V.E. Korepin, N.M. Bogoliubov, and A.Z. Izergin, *Quantum inverse scattering method and correlation functions* (Cambridge, Cambridge University Press, 1993).
[29] A.O. Gogolin, A.A. Nersesyan, and A.M. Tsvelik, *Bosonization and strongly correlated systems* (Cambridge, Cambridge University Press, 1998).
[30] T. Giamarchi, *Quantum physics in one dimension* (Oxford, Oxford University Press, 2004).
[31] U. Schollwöck, Rev. Mod. Phys. **77**, 259 (2005).
[32] N. Kitanine, K.K. Kozlowski, J.M. Maillet, G. Niccoli, N.A. Slavnov, and V. Terras, J. Stat. Mech. P10009 (2007); *ibid.* P07010 (2008).
[33] R.G. Pereira, J. Sirker, J.-S. Caux, R. Hagemans, J.M. Maillet, S.R. White, and I. Affleck, J. Stat. Mech. P08022 (2007).
[34] H.E. Boos, J. Damerau, F. Göhmann, A. Klümper, J. Suzuki, and A. Weiβe, J. Stat. Mech. P08010 (2008).
[35] F.H.L. Essler and R.M. Konik, J. Stat, Mech. P09018 (2009).
[36] N. Kitanine, K.K. Kozlowski, J.M. Maillet, N.A. Slavnov, and V. Terras, J. Stat. Mech. P04003 (2009); J. Math. Phys. **50**, 095209 (2009).
[37] A. Klauser, J. Mossel, J.-S. Caux, and J. van den Brink, Phys. Rev. Lett. **106**, 157205 (2011).
[38] K.K. Kozlowski and V. Terras, J. Stat. Mech. P09013 (2011).
[39] N. Crampe, E. Ragoucy, and D. Simon, J. Phys. A **44**, 405003 (2011).
[40] J. Sato, B. Aufgebauer, H. Boos, F. Göhmann, A. Klümper, M. Takahashi, and C. Trippe, Phys. Rev. Lett. **106**, 257201 (2011).
[41] A. Shashi, M. Panfil, J.-S. Caux, and A. Imambekov, Phys. Rev. B **85**, 155136 (2012).
[42] A. Luther and I. Peschel, Phys. Rev. B **12**, 3908 (1975).
[43] T. Hikihara and A. Furusaki, Phys. Rev. B **58**, R583 (1998); *ibid.* **69**, 064427 (2004).
[44] S. Lukyanov and A. Zamolodchikov, Nucl. Phys. B **493**, 571 (1997).
[45] S. Lukyanov, Phys. Rev. B **59**, 11163 (1999).
[46] B. Pozsgay, J. Stat. Mech. P11017 (2011).
[47] S.D. Glazek and K.G. Wilson, Phys. Rev. D **48**, 5863 (1993); *ibid.* **49**, 4214 (1994).
[48] F. Wegner, Ann. Phys. **3**, 77 (1994).
[49] A.L. Chernyshev, D. Galanakis, P. Phillips, A.V. Rozhkov, and A.-M.S. Tremblay, Phys. Rev. B **70**, 235111 (2004).
[50] J.-Y.P. Delannoy, M.J.P. Gingras, P.C.W. Holdsworth, and A.-M.S. Tremblay, Phys. Rev. B **72**, 115114 (2005).
[51] S. Müller, J. Billy, E.A.L. Henn, H. Kadau, A. Griesmaier, M. Jona-Lasinio, L. Santos, and T. Pfau, Phys. Rev. A **84**, 053601 (2011).
[52] A. Chotia, B. Neyenhuis, S.A. Moses, B. Yan, J.P. Covey, M. Foss-Feig, A.M. Rey, D.S. Jin, and J. Ye, Phys. Rev. Lett. **108**, 080405 (2012).
[53] C. Trefzger, C. Menotti, B. Capogrosso-Sansone, and M. Lewenstein, J. Phys. B **44**, 193001 (2011).
[54] T. Stöferle, H. Moritz, C. Schori, M. Köhl, and T. Esslinger, Phys. Rev. Lett. **92**, 130403 (2004).
[55] I.B. Spielman, W.D. Phillips, and J.V. Porto, Phys. Rev. Lett. **98**, 080404 (2007).
[56] G.G. Batrouni, V. Rousseau, R.T. Scalettar, M. Rigol, A. Muramatsu, P.J.H. Denteneer, and M. Troyer, Phys. Rev. Lett. **89**, 117203 (2002).
[57] V.A. Kashurnikov, N.V. Prokofev, and B.V. Svistunov, Phys. Rev. A **66**, 031601 (2002).
[58] G. Campbell, J. Mun, M. Boyd, P. Medley, A.E. Leanhardt, L.G. Marcassa, D.E. Pritchard, and W. Ketterle, Science **313**, 5787 (2006).
[59] S. Fólling, A. Widera, T. Müller, F. Gerbier, and I. Bloch, Phys. Rev. Lett. **97**, 060403 (2006).
[60] F. Gerbier, A. Widera, S. Fölling, O. Mandel, T. Gericke, and I. Bloch, Phys. Rev. Lett. **95**, 050404 (2005).
[61] D. Clément, N. Fabbri, L. Fallani, C. Fort, and M. Inguscio, Phys. Rev. Lett. **102**, 155301 (2009).
[62] L. Fallani, J.E. Lye, V. Guarrera, C. Fort, and M. Inguscio, Phys. Rev. Lett. **98**, 130404 (2007).
[63] T.D. Kühner, S.R. White, and H. Monien, Phys. Rev. B **61**, 12474 (2000).

[64] L. Amico and V. Penna, Phys. Rev. B **62**, 1224 (2000).

[65] V.W. Scarola and S. Das Sarma, Phys. Rev. Lett. **95**, 033003 (2005).

[66] D.L. Kovrizhin, G.V. Pai, and S. Sinha, Europhys. Lett. **72**, 162 (2005).

[67] G.G. Batrouni, F. Hebert, and R.T. Scalettar, Phys. Rev. Lett. **97**, 087209 (2006).

[68] T. Mishra, R.V. Pai, S. Ramanan, M.S. Luthra, and B.P. Das, Phys. Rev. A **80**, 043614 (2009).

[69] M.A. Cazalilla, R. Citro, T. Giamarchi, E. Orignac, and M. Rigol, Rev. Mod. Phys. **83**, 1405 (2011).

[70] R. Fazio and H. van der Zant, Phys. Rep. **355**, 235 (2001).

[71] G. Grignani, A. Mattoni, P. Sodano, and A. Trombettoni, Phys. Rev. B **61**, 11676 (2000).

[72] L.I. Glazman and A.I. Larkin, Phys. Rev. Lett. **79**, 3736 (1997).

[73] D. Giuliano and P. Sodano, Nucl. Phys. B **711**, 480 (2005).

[74] E. Altman and A. Auerbach, Phys. Rev. Lett. **89**, 250404 (2002).

[75] F.D.M. Haldane, Phys. Rev. Lett. **50**, 1153 (1983).

[76] H.J. Schulz, Phys. Rev. B **34**, 6372 (1986).

[77] E.G. Dalla Torre, E. Berg, and E. Altman, Phys. Rev. Lett. **97**, 260401 (2006).

[78] E. Berg, E.G. Dalla Torre, T. Giamarchi, and E. Altman, Phys. Rev. B **77**, 245119 (2008).

[79] L. Amico, G. Mazzarella, S. Pasini, and F.S. Cataliotti, New J. Phys. **12**, 013002 (2010).

[80] M. Dalmonte, M. Di Dio, L. Barbiero, and F. Ortolani, Phys. Rev. B **83**, 155110 (2011).

[81] D. Rossini and R. Fazio, New J. Phys. **14**, 065012 (2012).

[82] S. Eggert and I. Affleck, Phys. Rev. B **46**, 10866 (1992).

[83] S. Lukyanov and V. Terras, Nucl. Phys. B **654**, 323 (2003).

[84] Since only eigenstates with zero total spin along the z axis are physically meaningful (due to the constraint on the total number of particles), in the following we use the formulas of Ref. 43 at vanishing applied magnetic field.

[85] F. Mila and K.P. Schmidt, *Strong-Coupling Expansion and Effective Hamiltonians*, Chap. 19 of Ref. 2.

[86] J.K. Freericks and H. Monien, Phys. Rev. B **53**, 2691 (1996).

[87] Since $[S, \mathcal{P}] \neq 0$, H_I is different from $\tilde{H}_I = S^\dagger H_I S$.

[88] Although the contribution to the total energy arising from magnetic fields vanishes on the physical states due to the constraint on the particle number, in the intermediate calculations one has to retain it when computing the redefined XXZ parameters.

[89] Notice that, as discussed in the following, the constraint on the total number (implying that only states of the XXZ model with z-component of the total spin equal to zero may be realized within the BH model in the canonical ensemble) does not affect the spin-liquid - Néel-Ising phase transition, since it just implies the existence of (at least two) ferromagnetic domain walls, in the ferromagnetic-Ising phase of the XXZ model.

[90] S. Kehrein, *The flow equation approach to many-particle systems* (Berlin, Springer Verlag, 2006).

[91] This result does not depend on the particular choice of $r_{\max}$.

[92] M. Campostrini and E. Vicari, Phys. Rev. Lett. **102**, 240601 (2009); Phys. Rev. A **81**, 063614 (2010).

[93] J. Carrasquilla, F. Becca, A. Trombettoni, and M. Fabrizio, Phys. Rev. B **81**, 195129 (2010).

[94] I. Affleck, J. Phys. A **31**, 2761 (1998).

[95] In passing we point out that, to obtain more accurate results on the phase transition points, a finite-size scaling of the data with L is needed. Namely, one should estimate the value of $\Delta_{\text{eff}}^{AF/F}$ for different sizes L, and then perform a fit of that quantity with L, such to extrapolate the thermodynamic limit. This analysis lies beyond our present purposes, which are to provide estimates of the transition within a precision of $\approx 5\%$.

[96] Notice that computing the renormalization of the effective XXZ parameters via the Luttinger treatment done in Section IV with periodic boundary conditions is enough to give excellent agreement with BH numerical data, provided that, of course, the correlation functions of the XXZ are computed for open boundary conditions according to Eqs. (13)-(14).